GEOCHEMISTRY AND PROVENANCE OF THE EARLY PROTEROZOIC LIBBY CREEK GROUP, MEDICINE BOW MOUNTAINS, SOUTHEASTERN WYOMING

by
James G. Crichton

Submitted in partial fulfillment of the requirements for the degree of
Master of Science in Geochemistry

New Mexico Institue of Mining and Technology
Socorro, New Mexico
April, 1992

ABSTRACT

Although trace element distributions of fine-grained clastic sedimentary rocks have been increasingly used as provenance indicators, trace elements in coarser-grained sediments have received little attention as provenance indicators. In this study the effects of grain size on sediment geochemistry is evaluated by comparing related quartzites and pelites from the Early Proterozoic Libby Creek Group. The Libby Creek Group consists of quartzites, pelites, and diamictites which were deposited in a rifted basin along the southeastern margin of the Archean Wyoming Province. The main differences in major element distributions between the quartzites and pelites are a result of quartz dilution. Chondrite-normalized REE patterns of the Libby Creek sediments are typical of cratonic sediments. REE patterns are light REE-enriched and heavy REE-depleted with variable negative Eu anomalies. Sediments from the lower Libby Creek Group have small negative Eu anomalies while those from the upper part have negative Eu anomalies typical of Phanerozoic sediments. Trace element distributions are similar in quartzites and pelites except for Sc, Cr, Ni, and Co, which have very low concentrations in the quartzites. Trace element ratios commonly used as provenance indicators in shales (La/Sc, Th/Sc, Cr/Th, Ba/Co, Zr/Y and Zr/Cr) are highly variable in Libby Creek quartzites, even within the same formation. It is possible that intrastratal solution or hydraulic sorting of Fe-Ti oxides can explain the low metal contents and variable trace element ratios in the quartzites.

Mineral separates from a fuchsitic quartzite indicate that Th, U, Sc, Cr, Co and REE are mainly contained within mica. This suggests that most trace elements were contained in clay minerals in the original sediments. Zircon controls about 60% of the Hf, but only about 20% of the U and the heavy REE in the whole rock.

A change in provenance occurred between the deposition of the Medicine Peak Quartzite and Lookout Schist, and has been identified using trace elements. Mixing calculations indicate sediments from the Headquarters, Heart, and Medicine Peak Formations are derived from sources consisting of mainly TTG (tonalite-trondjehemite-granodiorite) and basalt, while the sediments from the Lookout Schist, Sugarloaf Quartzite, and French Slate are derived from sources containing large amounts of K-rich granites. The Libby Creek Group shows similar secular geochemical trends to other Early Proterozoic cratonic basin successions. These are likely related to progressive uplift and exposure of K-rich granites formed during the Late Archean. Using the geochemistry of the fine-grained sediments and the results obtained from mixing models, proposed values for the major and trace element composition of the Late Archean upper crust of the Wyoming Province are given.

Paleoweathering indices suggest that the climate changed from cold (glacial) during the deposition of the Headquarters Formation to tropical during the deposition of the French Slate.

Contents

ACKNOWLEDGEMENTS

I would like to thank Dr. Kent Condie for creating this project and guiding me carefully through it. A warm thanks also goes to my other committee members, Drs. Philip Kyle and Peter Mozley. Finally, I would like to thank Greg Hill and Scott McKitrick for reading a rough draft of this manuscript and providing many useful suggestions.

List of Figures

List of Tables

INTRODUCTION

Fine-grained clastic sedimentary rocks have been used in many studies to characterize the composition of their source areas and to demonstrate secular changes in the composition of the upper continental crust (Taylor and McLennan, 1985; Boryta and Condie, 1990; Wronkiewicz and Condie, 1987; 1989; 1990). Factors affecting the chemical composition of clastic sediments include source-rock composition, hydraulic sorting of minerals, adsorption of ions onto clay minerals, diagenesis (specifically intrastratal solution), and degree of source-area weathering (Sawyer, 1986; Wronkiewicz and Condie, 1987). Redistribution of elements during metamorphism can also alter rock composition. In order to properly characterize the source-areas of detrital sediments, the effects of each of these processes must be evaluated. Shales and their metamorphic equivalents have typically been used in geochemical provenance studies because many of the above variables are minimized or at least are more easily identified than they are for coarser-grained sediments (siltstones, sandstones, and conglomerates).

Traditionally, provenance studies involving coarser-grained clastic sedimentary rocks have focused on petrography. The accuracy of these studies is suspect, even for unmetamorphosed rocks, due to the possible effects of diagenesis on detrital modes. Diagenetic alterations of detrital modes may include dissolution of unstable grains, replacement of grains (e.g. albitization of plagioclase), and transformation of labile components into matrix (Blatt, 1985; Mcbride, 1985; Milliken, 1988; Pittman, 1979; Helmhold, 1985). Due to the possible problems of using detrital modes as provenance indicators and because shales are not always available for chemical analysis, provenance investigations involving whole-rock

chemistry of coarser-grained sediments are warranted. Few studies have used major and trace element chemistry of sandstones or their metamorphic equivalents as provenance indicators (van de Kamp and Leake, 1986; Denis and Dabard, 1988). In these studies, shales are either not present or were not sampled; therefore, the effect of grain size on sediment chemistry cannot be evaluated. As such, the significance of using whole-rock chemistry of coarser clastics in geochemical provenance studies has yet to be fully evaluated.

The present study contributes to an understanding of the whole-rock chemistry of coarser sediments as provenance indicators by considering a lithologically mixed (pelites, diamictites and quartzites) group of sediments deposited in a passive-continental margin tectonic setting. Through comparison of elemental distributions between closely related quartzites and pelites, the effects of grain size on sediment composition are evaluated. The Early Proterozoic Libby Creek Group is ideal for this type of study and is especially attractive because of a detailed sedimentological study published on the succession by Karlstom et al. (1983).

Another objective of this study is to test the proposition by Taylor and McLennan (1983; 1985) that a major change in the Late Archean upper crustal composition is recorded in Early Proterozoic clastic sediments. Some Early Proterozoic basin successions (the Huronian which is exposed along the north shore of Lake Huron, Canada and the Pine Creek Geosyncline located in Australia) show increases in the size of the negative Eu anomaly, total REE contents, Th and U contents and decreases in Sc, Co, Cr, and Ni contents with increasing stratigraphic height (Taylor and McLennan, 1983; 1985). These changes in sediment composition have been

ascribed to unroofing of Late Archean K-rich granites (McLennan et al., 1979).

The present study shows that many of the trace elements useful in determining the provenance of shales are equally useful in coarser-grained clastic sediments and can provide more detailed information on source-area composition than can be obtained from detrital modes. Chemical analysis of mineral separates of a quartzite allows the locations of many trace elements to be determined, and provides important constraints on provenance. The Libby Creek Group also shows many geochemical trends that are similar to those present in other Early Proterozoic basin successions.

General Geology

The Libby Creek Group forms the upper part of the Snowy Pass Supergroup, which is located in the Medicine Bow Mountains in southeastern Wyoming (Fig. 1). The Libby Creek Group overlies older, more complexly deformed metasediments of the Deep Lake Group and the Phantom Lake Metamorphic Suite. The base of the Libby Creek Group is in thrust fault contact with the Deep Lake Group, whereas the upper portion abuts the Cheyenne Belt (Fig.1). The Cheyenne Belt is a major shear zone that separates the Archean Wyoming province to the north from younger accreted island arc terranes to the south.

The depositional age of the lower Libby Creek Group is reasonably well constrained. Pegmatites in the Deep Lake Group have been dated at 2.1 Ga providing an upper limit on the depositional age, whereas an intrusive into the lower Libby Creek Group has been dated at 2.0 Ga. Therefore, the lower Libby Creek Group must have been deposited between 2.1 and 2.0 Ga. The

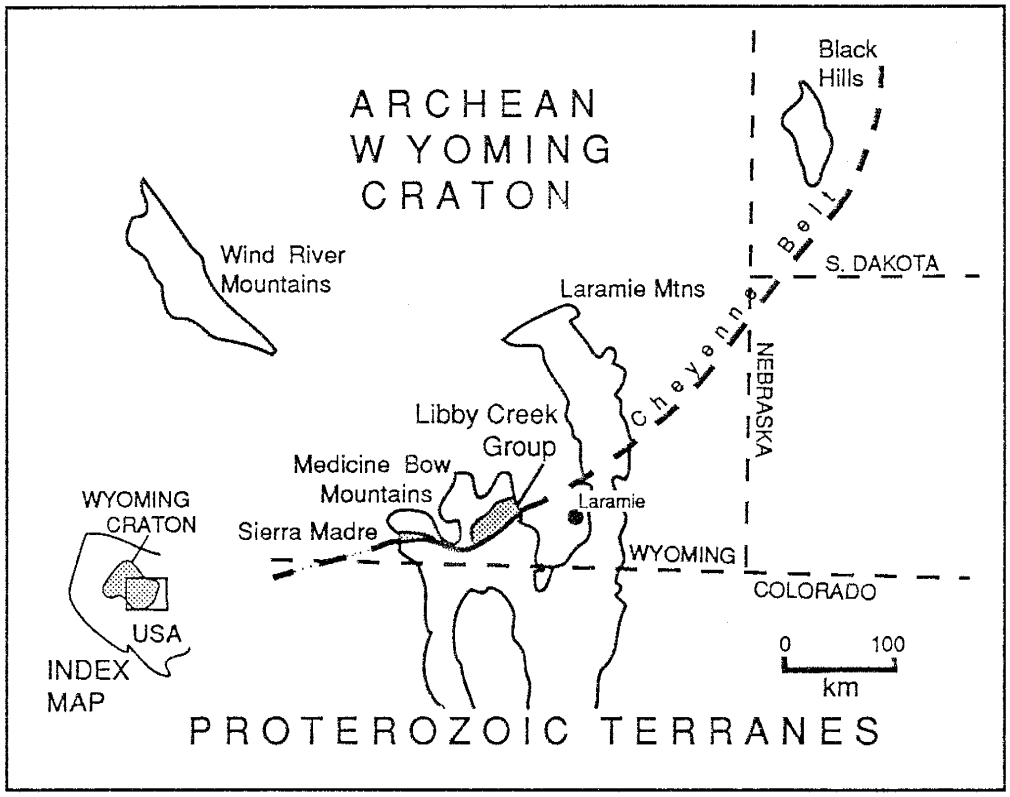

Figure 1. Location map showing the Early Proterozoic Libby Creek Group along the southeastern margin of the Archean Wyoming Province.

depositional age of the upper Libby Creek Group is not as well constrained, but must be older than initial shearing along the Cheyenne Belt which occurred at 1.8 Ga (Premo and Van Schmus, 1989).

The Libby Creek Group consists of approximately 7.5 km of deformed metasediments (Karlstom et al., 1983), with bedding steeply dipping to vertical. Metamorphic grade increases stratigraphically upward from the chlorite zone of the greenschist facies to upper amphibolite facies for portions of the French Slate, which are in close proximity to the Cheyenne Belt (Duebendorfer, 1988; Duebendorfer and Houston, 1987). This inverted metamorphic gradient has been attributed to loading associated with tectonic activity along the Cheyenne Belt. Hills et al. (1968) placed a minimum metamorphic age of 1710 ± 60 Ma for the Libby Creek Group, using whole rock Rb/Sr isochrons of the metasediments. This age is coincidental with D_2 thrusting along the Cheyenne Belt (Duebendorfer and Houston; 1987, Duebendorfer, 1988).

The Libby Creek Group was deposited in a rifted basin along the southeastern margin of the Archean Wyoming Province. The Deep Lake Group and the Libby Creek Group represent a transgressional sequence with their source rocks to the north and east as is indicated by paleocurrent data (Karlstrom et al., 1983). Due to the presence of a rotated thrust fault in the Libby Creek Group, Karlstrom et al. (1983) divided the group into lower and upper portions, which also represent different depositional environments (Fig. 2). The depositional environment of the lower Libby Creek Group is interpreted to be glaciomarine-deltaic whereas that of the upper Libby Creek Group is thought to be intertidal to deep marine (Karlstrom et al., 1983). The lowest stratigraphic unit considered in this study is the Headquarters Formation. It is lithologically variable

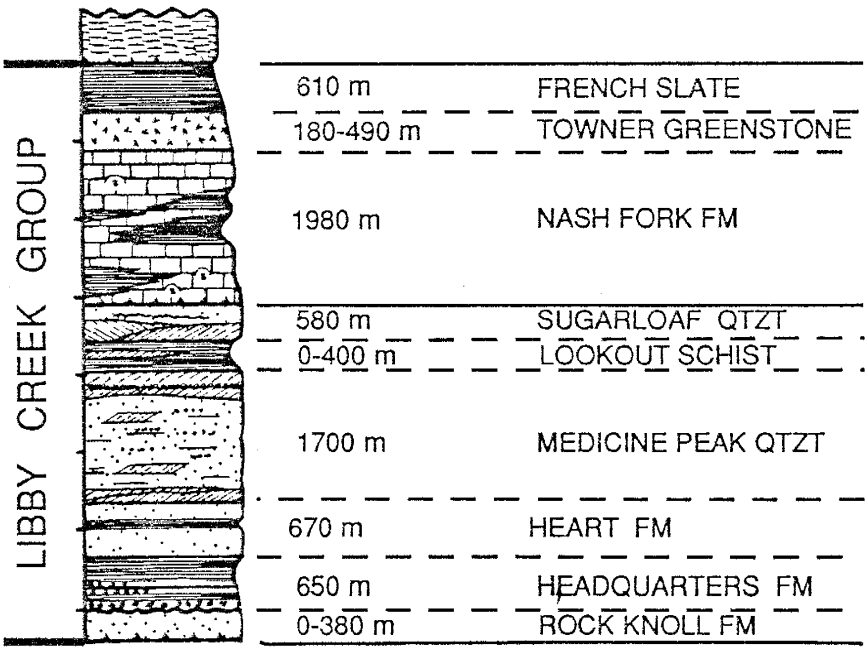

Figure 2. Generalized stratigraphic section of the Libby Creek Group (modified after Karlstrom et al. 1983).

containing paraconglomerates, phyllites, laminated schist, and quartzites (Karlstrom et al., 1983). The Headquarters Formation is considered to be glaciomarine with the paraconglomerates representing diamictites. Varved units may also be present. The Heart Formation consists mainly of fine to medium-grained quartzites which become coarser near the top of the formation. It is thought to have been deposited in a deltaic setting on a tide-dominated delta (Karlstrom et al.,1983). The Medicine Peak Quartzite is a thick (2000m) medium to coarse-grained quartzite thought to have been deposited in an estuary (Karlstrom et al.,1983). It is interesting to note that Kauffman and Steidtmann (1981) have observed sedimentary structures in the Medicine Peak Quartzite that appear to be metazoan trace fossils, and if so, they may be the oldest evidence of metazoans. The Lookout Schist is a lithologically variable unit consisting of phyllites, arkoses and quartzites with a depositional environment similar to that of the Heart Formation (Karlstrom et al., 1983). The Sugarloaf Quartzite is a mature medium-grained quartz arenite. The maturity of this unit led Karlstrom et al., (1983) to interpret it to have been deposited in a shallow marine environment.

As mentioned above the upper Libby Creek Group is in thrust fault contact with the lower Libby Creek Group. The base of the upper Libby Creek Group is defined by the Nash Fork Formation (Fig. 2). It is a thick (2000m) metadolomite unit containing beds of phyllite. Large botryoidal stromatolites occur throughout the Nash Fork Formation, and it is therefore interpreted to have been deposited in an intertidal environment (Karlstrom et al., 1983). The Towner Greenstone, not sampled in this study, is thought to be mafic pyroclastic deposits and represents the only volcanic rocks in the Libby Creek Group. The uppermost formation of the Libby

Creek Group is the French Slate (Fig. 2). It consists mainly of black slate, but also contains small quartzite beds at its base and minor iron formation (Karlstrom et al.,1983). It is believed to have been deposited in a low-energy marine environment.

The striking similarity between the Libby Creek sediments and the Huronian sediments was noted in the first serious geological investigation of the Medicine Bow Mountains (Blackwelder, 1926). Workers have since proposed correlations between them (Young, 1970; Roscoe, 1989). The similar ages and excellent unit for unit matches between the Libby Creek Group and the Huronian may indicate that the Libby Creek and the Huronian are equivalent. However, recent isotope work suggests that the Wyoming and Superior cratons were separated until about 1.9 Ga (Hoffman, 1989). Since most deposition occurred before this time it is very unlikely that that the Libby Creek and the Huronian were laterally continuous.

Methods

Field work was performed during the summer of 1990. Representative metasedimentary samples from the Libby Creek Group were collected and sample sites are shown on Figure A-1 in Appendix A. Sampling was concentrated in the central Medicine Bow Mountains where the Libby Creek Group is well exposed in the cores of eroded anticlines. Thin-sections of representative samples were made for petrographic study, and minerals were separated from one sample using heavy liquids and hand-picking techniques. Each separated phase was analyzed by INAA (Instrumental Neutron Activation Analysis).

Chemical analyses were made of 38 whole rock samples by INAA and XRF (X-ray Fluorescence) methods. For the INAA method, samples were irradiated at Sandia National Laboratory in Alberquerque, New Mexico with the abundances of Hf, Ta, Sc, Co, Ni, Cr, Ba, Th, U, Cs, and seven REE being obtained at New Mexico Tech using gamma-ray detectors and data reduction software. Major elements and Rb, Sr, Y, Zr, and Nb were obtained by XRF also at New Mexico Tech using a Rigaku XRF Spectrometer. For a complete description of sampling, sample preparation and analytical procedures refer to Appendix A.

Petrographic Results

A total of 14 thin-sections were made from the Libby Creek sediments and modal analyses were made using standard point counting methods (Pettijohn et al., 1973)(Table 1). Quartzites and quartz-rich pelites from the Headquarters and Heart Formations contain 50-80% quartz, 20-50% mica and 1-3% plagioclase with minor amounts of zircon, Fe-Ti oxides and apatite. Karlstrom et al. (1983) reported K-feldspar and plagioclase arkoses from the Headquarters Formation, and they also observed sphene and tourmaline in the quartzites. Pelites from the Headquarters and the Heart Formations are composed of biotite, chlorite and quartz with similar minor phases as the quartzites. The diamictites from the Headquarters Formation are poorly sorted consisting of a fine-grained matrix with sporadic cobble to boulder-sized clasts. The matrix consists of quartz, feldspar, rock fragments, and mica in varying proportions. The large clasts are granitoids, quartzites and schist with most 4 to 6 cm in diameter, but some are as large as 1 meter. The average size of these clasts increases to the east, indicating ice movement from that direction (Lanthier, 1979).

Table 1. Modal analyses of selected Libby Creek quartzites.

Sample	Quartz	Mica	Plag.	Fe-Ti oxides	Other minor phases	Miscellaneous
FS15	94	minor		2		4 - carbonate
SL42	99	minor		1		
SL72	99	1		minor		
SL7E	98	2		minor		
SL7F	98	2				
LS32	98	2		minor		
LS53	95	1	1	1	zircon	2 - rock frags.
MP1	83	17			sphene > zircon	
MP2	85	15			sphene > zircon	
MP91	96	4			amphibole?	
MP96	99	1		minor		
MP112	97	3			zircon	
H101	73	24	2	1		
HQ62	55	45	minor	minor	amphibole?	

Phases are reported as a percent of the whole rock. 200 - 500 points were counted on each thin section. The Petrographic Results Section is a summary of this material and that of Karlstrom et al. (1983). FS = French Slate, SL = Sugarloaf Quartzite, LS = Lookout Schist, MP = Medicine Peak Quartzite, H = Heart Formation, HQ = Headquarters Formation.

The majority of the granitoid clasts collected in this study appear to be tonalites with very few granites (sensu strictu) being represented. The quartzite clasts studied are mineralogically mature, medium-grained, white quartz arenites. Due to sampling problems, only diamictite matrices were chemically analyzed.

The Medicine Peak Quartzite consists of mineralogically mature, medium to coarse-grained quartzites. Samples studied consisted of 83-99% quartz, 1-17% mica, and minor amounts of zircon, sphene and opaques. The mica is typically muscovite although in two samples (MP1 and MP2) it is fuchsite. Sphene occurs as idiomorphic crystals which crosscut quartz and mica grains, suggesting a metamorphic origin. Feldspar and rock fragments are absent in this formation, however it does contain an unusual suite of aluminosilicate minerals (sericite, pyrophyllite and kyanite).

Quartzites studied from the Lookout Schist contain 95-98% quartz, 0-1% plagioclase, 0-3% rock fragments and 1-2% mica, with trace amounts of zircon, apatite and Fe-Ti oxides (Table 1). Pelites and arkoses from the Lookout Schist studied by Karlstrom et al. (1983) consist of variable amounts of quartz, sericite, plagioclase, orthoclase, chlorite, biotite, and calcite with minor amounts of Fe-Ti oxides, zircon and tourmaline.

The Sugarloaf Quartzite consist of mineralogically mature, medium-grained quartzites. Samples contain 97-99% quartz, 0-2% mica and minor amounts of Fe-Ti oxides. Although most of the quartz is recrystallized, some grains still show a high degree of rounding.

The pelites of the French Slate consist of layers with subequal amounts of muscovite, chlorite, quartz, and minor Fe-Ti oxides alternating with quartz-rich, mica-poor layers (Karlstrom et al., 1983).

GEOCHEMICAL RESULTS

Major Elements

The detrital sediments sampled from the Libby Creek Group range in composition from pelites with SiO_2 contents of 63 to 85% and Al_2O_3 contents of 7 to 17% to quartzites with SiO_2 contents of 90 to 99% and Al_2O_3 contents of only 1 to 6.5%. A strong negative correlation exists between SiO_2 and Al_2O_3 (Fig. 3). Compositional gaps occur at 70 and 90% SiO_2 with the corresponding Al_2O_3 gaps at 14 and 7%, respectively. These compositional gaps probably reflect incomplete sampling, not primary sedimentary differentiation. Strong negative correlations also exist between SiO_2 and Fe_2O_3, TiO_2, MgO, and K_2O with a gap at about 90% SiO_2 for these distributions. As expected, these elements are positively correlated with Al_2O_3 and a gap occurs at about 7% Al_2O_3 for these distributions. The compositional gaps on SiO_2 variation diagrams at about 90% SiO_2 provide a convenient though arbitrary division between pelites and quartzites of the Libby Creek Group and this terminology will be used throughout this study.

Pelites from the Libby Creek Group are depleted in most major elements relative to average Phanerozoic shales represented by PAAS (Post Archean Average Shale; Taylor and McLennan, 1985). They have higher SiO_2 contents and lower Al_2O_3 contents than PAAS (Fig. 4), probably a result of quartz dilution. This is also indicated by the negative major element correlations observed on SiO_2 variation diagrams. While the quartz dilution effect is relatively small in the pelites, quartzites have major elements contents (except SiO_2) 5 to 6x less than PAAS. Major element distributions of the pelites is similar to PAAS, disregarding quartz dilution effects, except for the behaviour of Na and Ca (Fig. 4). Pelites from the

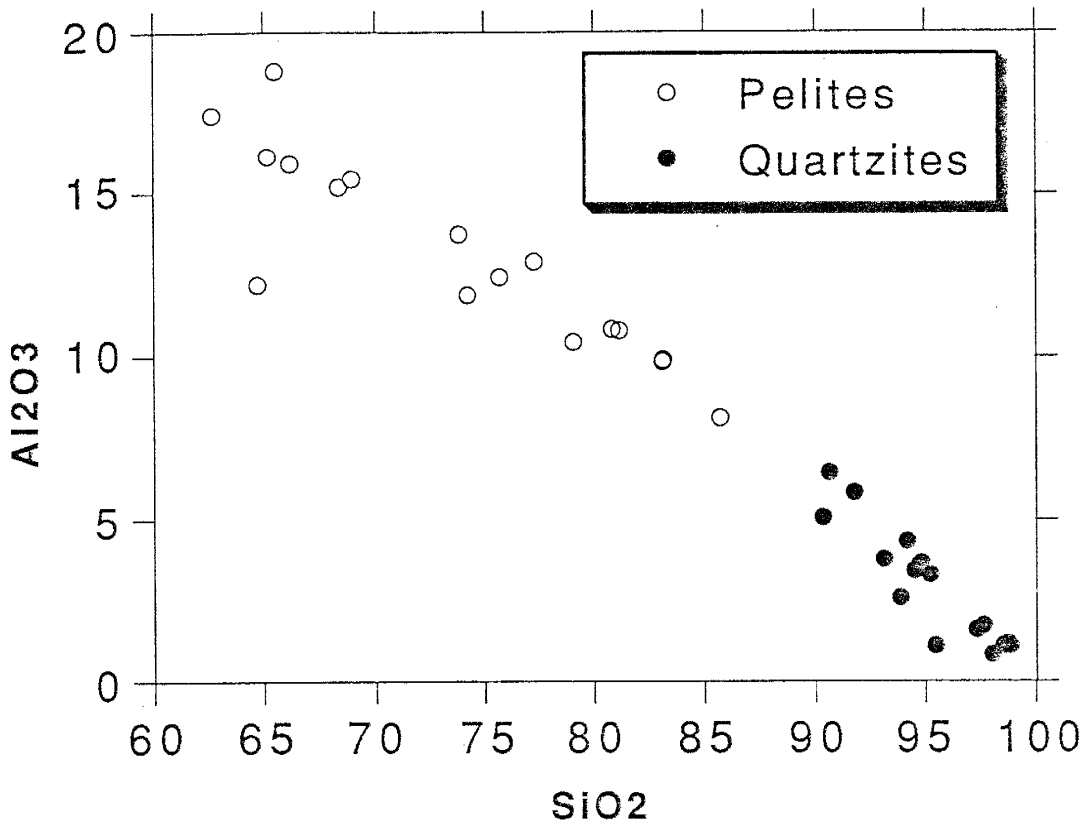

Figure 3. Al_2O_3 versus SiO_2 diagram for clastic sediments from the Libby Creek Group. The gap between 85 and 90% SiO_2 is used to separate the pelites from the quartzites.

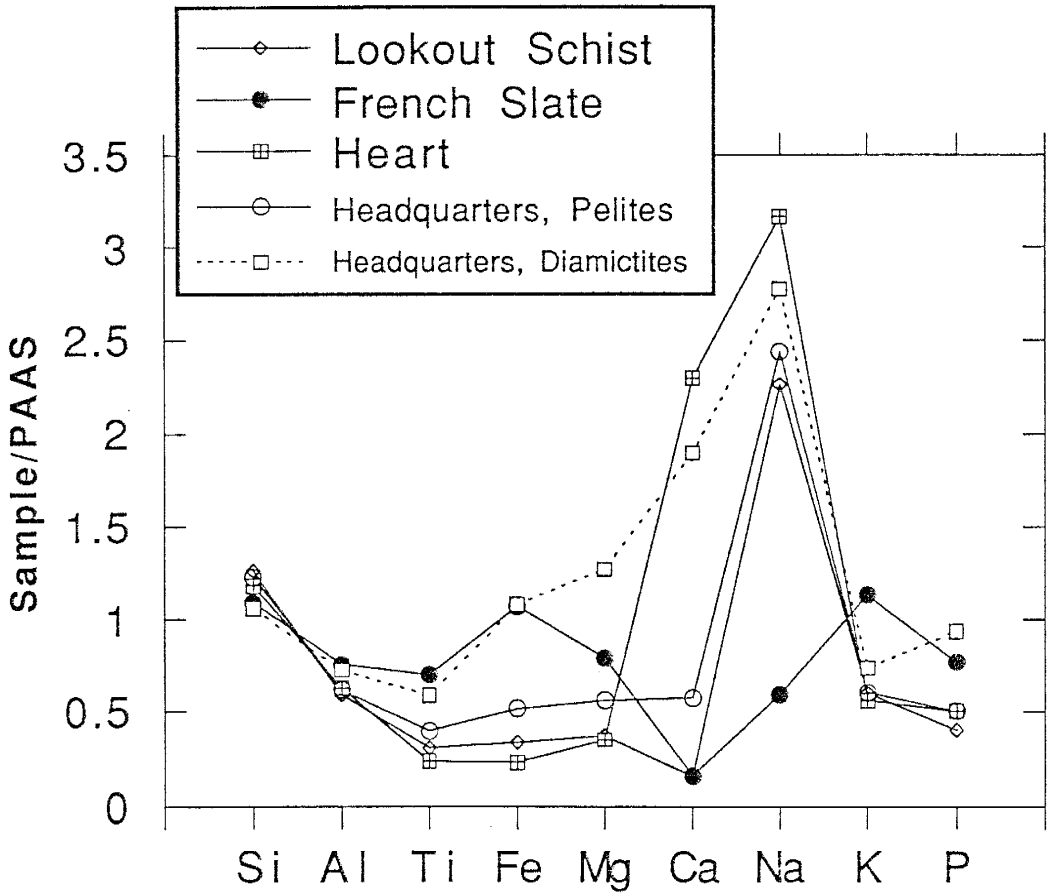

Figure 4. Major elements normalized to PAAS for pelite and diamictite averages from the Libby Creek Group. PAAS (Post Archean Average Shale) (Taylor and McLennan, 1985) composition is given in Appendix C. Formation averages and standard deviations are also given in Appendix C.

Headquarters Formation and Lookout Schist are enriched in Na and depleted in Ca, whereas diamictites from the Headquarters Formation and pelites from the Heart Formation are enriched in both Na and Ca relative to PAAS (Fig. 4). Pelites from the French Slate have Na values similar to PAAS, but Ca is about 6x less. The variable enrichment of Na and Ca likely reflects variable amounts of detrital plagioclase in these sediments, which is a function of their relative immaturity. Calcite cement may also increase the Ca content. The decoupling of Na and Ca observed in pelites from the Headquarters Formation, Lookout Schist, and French Slate may indicate that Ca-rich feldspar is less stable during weathering than Na-rich feldspar and/or that plagioclase loses Ca in preference to Na during weathering (Clayton, 1986). Another possible explanation is diagenetic albitization of feldspar, which is common in sandstones but has also been observed in shales (Blatt, 1985). It is also possible, but not likely, that this is a TTG (tonalite-trondjehemite-granodiorite) effect. Archean TTG has high Na contents relative to Ca, therefore the apparent decoupling of Na from Ca in the Libby Creek sediments could derived from the source-rocks. However, both the French Slate and Lookout Schist are likely derived from source-areas containing small amounts of TTG (discussed later).

The K_2O/Na_2O ratio varies from low values in fine-grained sediments from the Headquarters and Heart Formations (0.4 to 1.8) to relatively high values in the French Slate (4 to 9) (Table B-1). Again this variation is likely a function of the maturity of these sediments as K is incorporated into clay minerals produced during the weathering of orthoclase. This is indicated by the similar Al_2O_3/K_2O ratios in the Libby Creek sediments to that of illite (Fig. 5). Two quartzites deviate from this distribution suggesting secondary loss of K. In contrast to K, Na released by weathering of plagioclase is lost

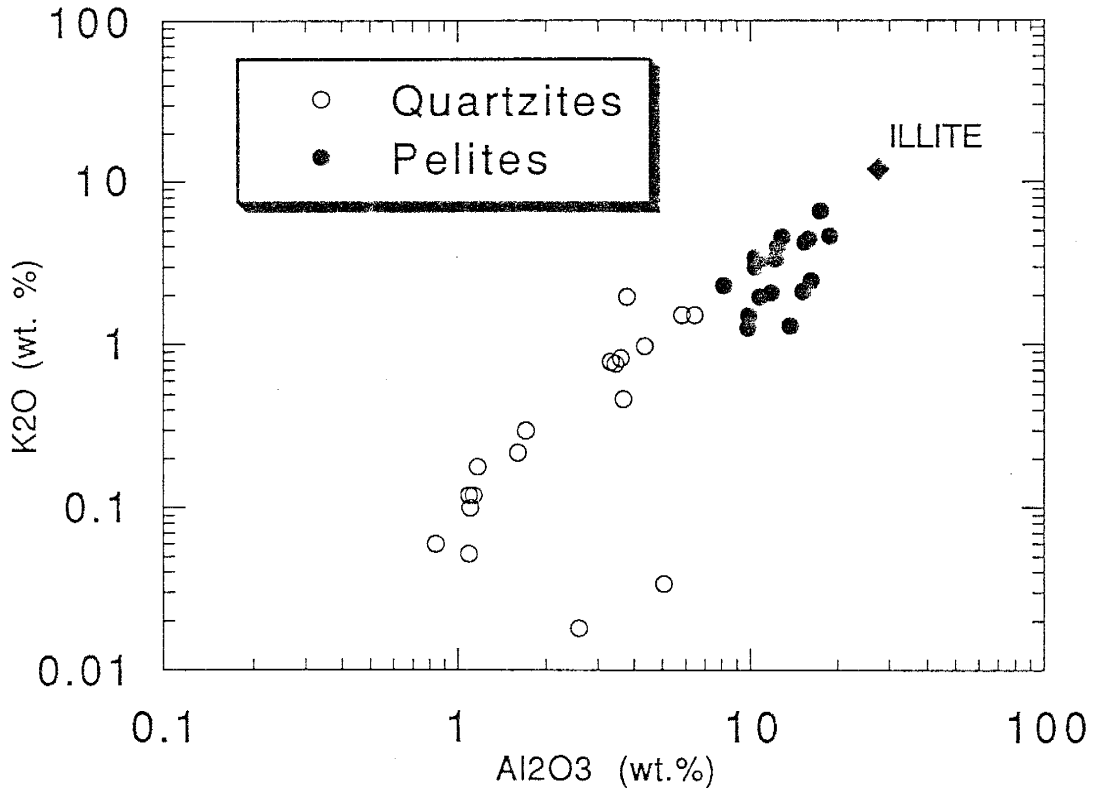

Figure 5. K_2O versus Al_2O_3 diagram for the clastic sediments from the Libby Creek Group.

from the system (Nesbitt et al., 1980). The quartzites have low K_2O/Na_2O ratios (0.01 to 2), which probably reflects the small amounts of mica (originally clay minerals) and K-feldspar present in the quartzites and consequently low K.

Al_2O3/TiO_2 and Al_2O_3/Fe_2O_3 ratios are considerably more variable and are generally higher in the quartzites than in associated pelites (Figs. 6a, 6b). This could reflect diagenetic loss of Fe-Ti oxides through intrastratal solution. Fe-oxides are known to be unstable during diagenesis, with Fe-Ti oxides becoming more stable as the Ti content increases (Miliken and Mack, 1990). Variable post depositional removal of these minerals could account for the variable Fe and Ti contents of the quartzites. Conversely, this variability might be a primary feature. It is possible that the Fe-Ti oxides followed clay minerals during transportation and deposition, thus depleting the original sands in these minerals. This has been documented for Fe-oxides (Carroll, 1958).

Trace Elements

Most trace elements in Libby Creek sediments are depleted relative to Phanerozoic shales (PAAS), reflecting variable amounts of quartz dilution. Inverse correlations between SiO_2 and many trace elements also suggest a quartz dilution effect. In order to facilitate comparisons between formations and lithologies, all samples have been normalized to PAAS. On the PAAS-normalized diagrams the trace elements are arranged in order of increasing compatibility with respect to average Archean granite (liquid) assumed to have been derived from partial melting of average Archean upper continental crust. These are not equivalent to bulk distribution coefficients in that the source composition (upper continental crust) is used

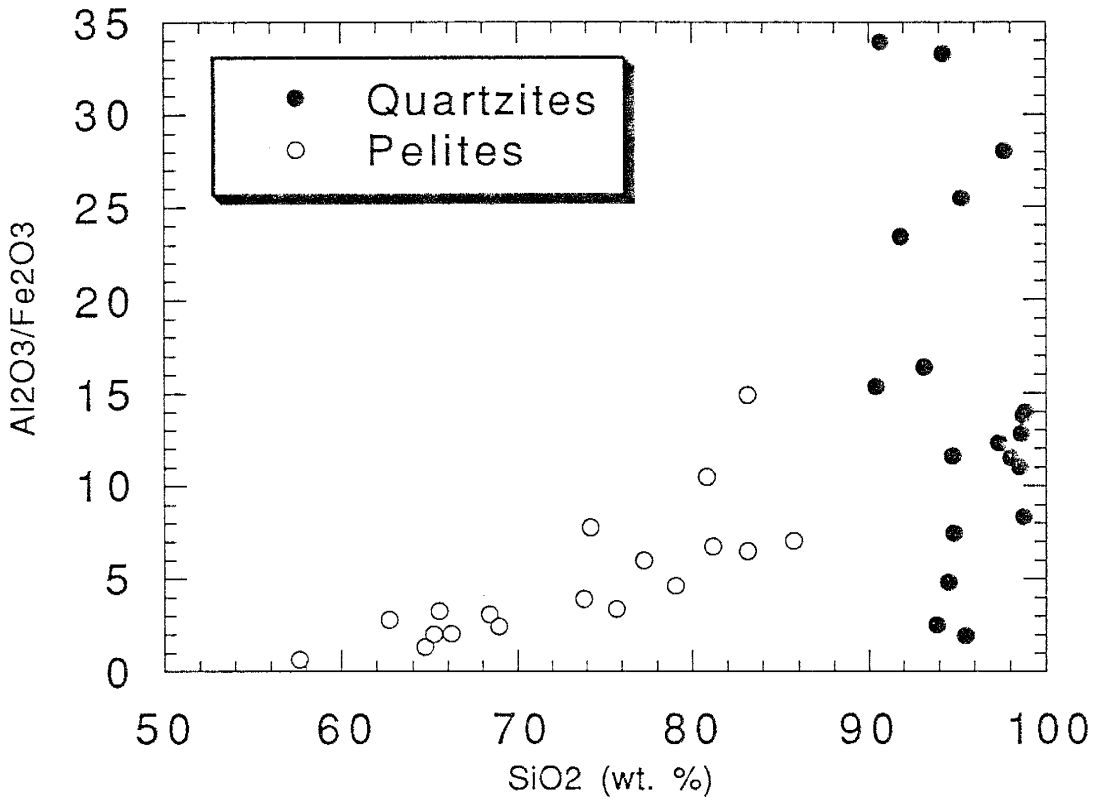

Figure 6a. Al_2O_3/Fe_2O_3 versus SiO_2 diagram for the clastic sediments of the Libby Creek Group.

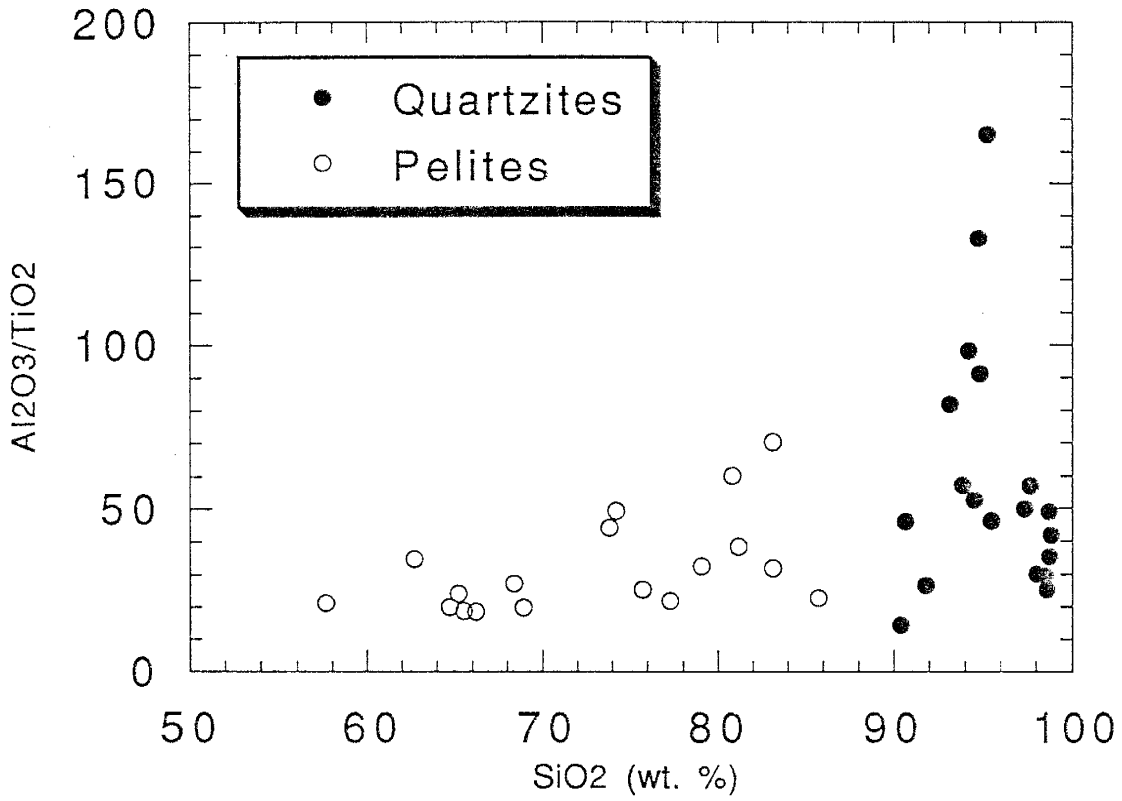

Figure 6b. Al_2O_3/TiO_2 versus SiO_2 diagram for the clastic sediments of the Libby Creek Group.

in place of restite composition. Relative to Eu and Sc, pelites from the Lookout Schist and French Slate show strong Sr depletion while pelites and diamictites from the Headquarters and Heart Formations show little or no Sr depletion (Figs. 7, 9). Conversely, Sr depletion is observed in quartzites from the Medicine Peak Quartzite and Lookout Schist (Figs. 8, 9). The Sr depletion is likely related to paleoweathering effects and is discussed in a later section. A negative Ba anomaly is observed for quartzites from the Heart, Medicine Peak, Lookout, and Sugarloaf Formations while no Ba anomaly is present in the pelites from any formation or quartzites from the Headquarters Formation (Figs. 7, 8, 9). The low Ba content in most of the quartzites may be related to the destruction of feldspars, which are known to concentrate Ba, in the quartzites and may be a function of their high permeability. Conversely, the low Ba content may be explained by low feldspar content in the original sands. Th/U ratios in the fine-grained sediments are typical of Phanerozoic shales (PAAS = 4.7) and are relatively constant (3.7 to 6.0) whereas Th/U ratios in the quartzites are highly variable (1.2 to 10) (Tables B-1, B-2). The variability of Th/U in the quartzites is controlled largely by U and is probably due to the higher solubility of U relative to Th (McLennan and Taylor, 1980) and the permeable nature of the quartzites. This variability may also suggest Th and U have different mineralogic controls in the quartzites and are hence decoupled.

Zr/Hf ratios in the Libby Creek sediments vary from 30 to 53 with most samples falling around 40. This is similar to the Zr/Hf ratio of the upper crust (Taylor and McLennan, 1985). Pelites from the Headquarters and Heart Formations show Zr enrichments on a PAAS-normalized diagram (Fig. 7), which may reflect variable zircon concentration in these samples. Zr enrichment is also observed in quartzites from the Heart, Medicine Peak

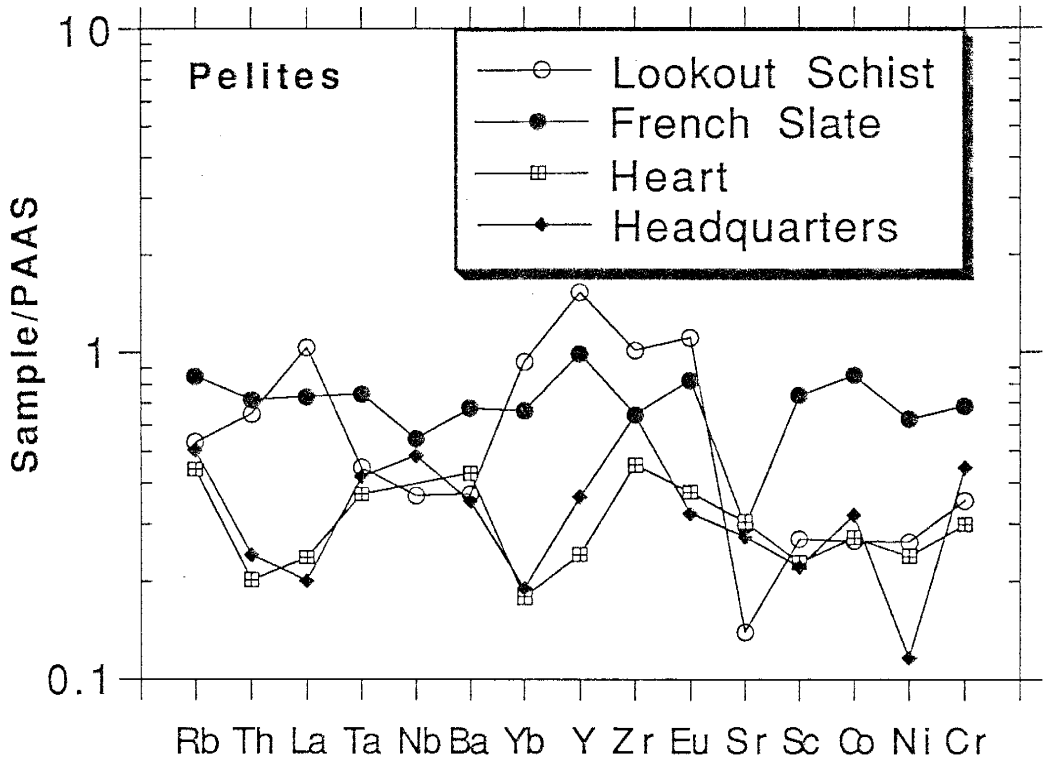

Figure 7. PAAS-normalized trace element distributions for the Libby Creek pelites. See text for ordering of elements. PAAS (Post Archean Average Shale) (Taylor and McLennan, 1985) composition given in Appendix C. Formation averages and standard deviations are also given in Appendix C.

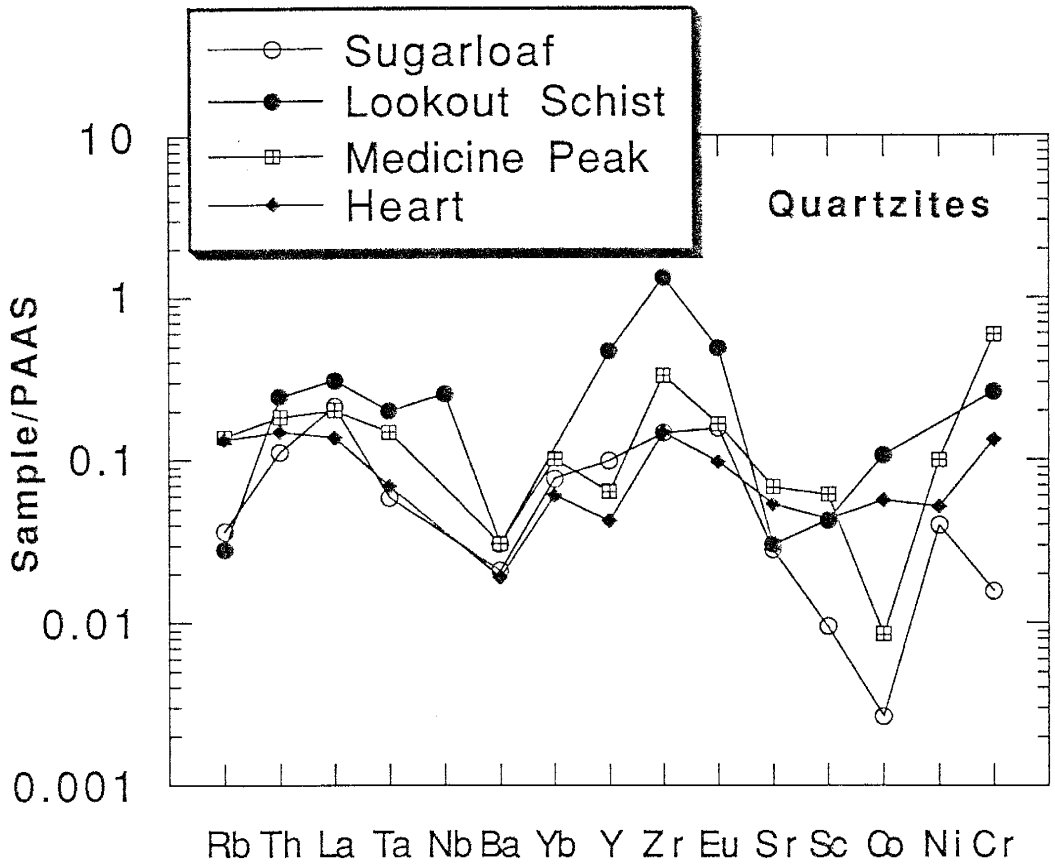

Figure 8. PAAS-normalized trace element distributions for quartzite averages by formation. See text for ordering of the elements. PAAS (Post Archean Average Shale) (Taylor and McLennan, 1985) composition given in Appendix C. Formation averages and standard deviations are also given in Appendix C.

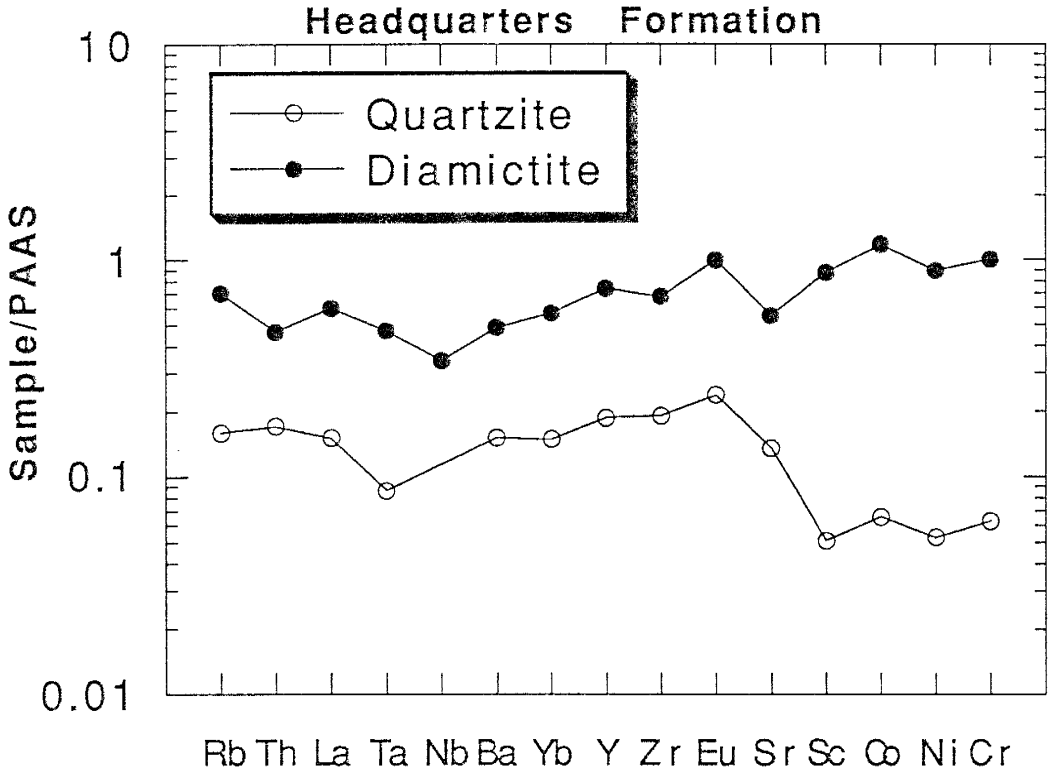

Figure 9. PAAS-normalized trace element distributions for quartzite and diamictite averages from the Headquarters Formation. See text for ordering of the elements. PAAS (Post Archean Average Shale) (Taylor and McLennan, 1985) composition given in Appendix C. Formation averages and standard deviations are also given in Appendix C.

and Lookout Schist Formations (Fig. 8). The lack of correlation between Zr and REE or Th indicate that zircon is not important is controlling REE and Th distributions in the Libby Creek sediments.

Fine-grained sediments from the Libby Creek Group have low Cr (< 115 ppm) and Ni (< 50 ppm)(Table B-1) contents which is typical of post-Archean shales. For comparison, Archean shales often contain several thousand ppm Cr and up to 1000 ppm Ni (Maas et al., 1991; Wronkiewicz and Condie, 1987). The Cr/Th ratios of the fine-grained sediments from the Headquarter and the Heart Formations are higher than those from the Lookout Schist and French Slate. The high Cr/Th ratio in the Headquarters and Heart Formations is controlled by both higher Cr and lower Th contents relative to the pelites from the Lookout Schist and French Slate. Most quartzites have very low Cr/Th ratios (as low as 0.8) which is due to the low Cr content of the quartzites. La/Sc and Th/Sc ratios are similar in fine-grained sediments from all formations (La/Sc = 1.2 to 2.6; Th/Sc = 0.38 to 1.2) and are similar to Phanerozoic shales (PAAS, La/Sc = 2.4; Th/Sc = 0.91). These ratios are much more variable in the quartzites and are generally higher (La/Sc up to 90 and Th/Sc up to 20). This variability is a result of the low Sc contents of the quartzites. On PAAS-normalized diagrams for the quartzites, Sc, Co, Ni, and Cr are depleted relative to Th, REE and some HFSE (High Field Strength Elements) (Figs. 8, 9). For quartzites and diamictites from the Headquarters Formation, the trace element distributions are identical except for Sc, Co, Ni, and Cr which are depleted in the quartzites (Fig. 9). The depletion of these elements in the quartzites may be a result of diagenetic loss or low original content of Fe-Ti oxides which is discussed later. In the quartzites from the Medicine Peak and Heart Formations, Cr is enriched relative to Sc, Co, and Ni. This may

indicate that in the original sediments, Cr was contained in clay minerals, as is suggested by fuchsite in the Medicine Peak Quartzite, and was decoupled from Sc, Co, and Ni, which may have been contained dominantly in other phases.

REE Distributions

Chondrite-normalized REE patterns of the Libby Creek sediments are typical of cratonic sediments (Fig. 10a- f). REE patterns are LREE enriched and HREE depleted with variable negative Eu anomalies. Most Libby Creek pelites have LREE contents of 100x chondrites and HREE contents of 10x chondrites. This is similar to Phanerozoic shales (PAAS), but subtle differences are observed. The La_n/Sm_n ratio of the pelites is relatively constant ranging between 3.0 to 3.5, which is 1.1 to 1.3x lower than PAAS. The La_n/Yb_n ratios of the pelites are 1 to 1.3x greater than PAAS, whereas the Gd_n/Yb_n ratios are 1.2 to 1.5x greater than PAAS. This indicates that Libby Creek pelites are depleted in HREE relative to Phanerozoic shales. This may reflect more Archean TTG (tonalite-trondjehemite-granodiorite) input into the Libby Creek sediments, as TTG is commonly enriched in the LREE and is always depleted in the HREE relative to other igneous rocks. Variability in the size of the negative Eu anomaly is also observed. Pelites and diamictites from the Headquarters and Heart Formations have small negative Eu anomalies ($Eu/Eu^* = 0.84$ to 0.93 whereas pelites from the Lookout Schist and French Slate have larger negative Eu anomalies ($Eu/Eu^* = 0.48$ to 0.71).

Quartzites of the Libby Creek Group have similar slopes on chondrite-normalized REE diagrams as do associated pelites, but REE concentrations are typically 5 to 6x less due to quartz dilution (Fig. 10 b-f). The similar

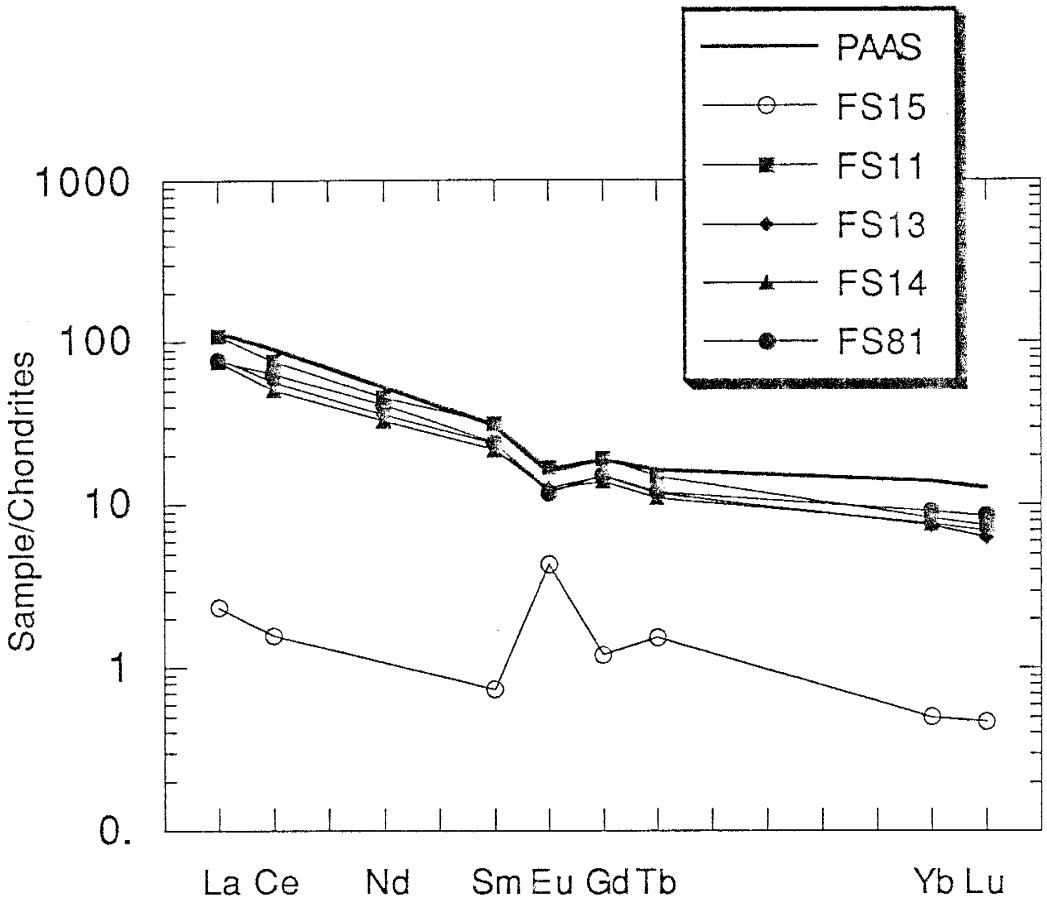

Figure 10a. Chondrite-normalized REE distributions for representative samples from the French Slate. Pelites are shown with filled symbols while the quartzite has an open symbol. Chondrite values are from Haskin et al. (1968) and are given in Appendix C. Gd is estimated by $Gd_n = (Sm_n \times Tb_n^2)^{1/3}$.

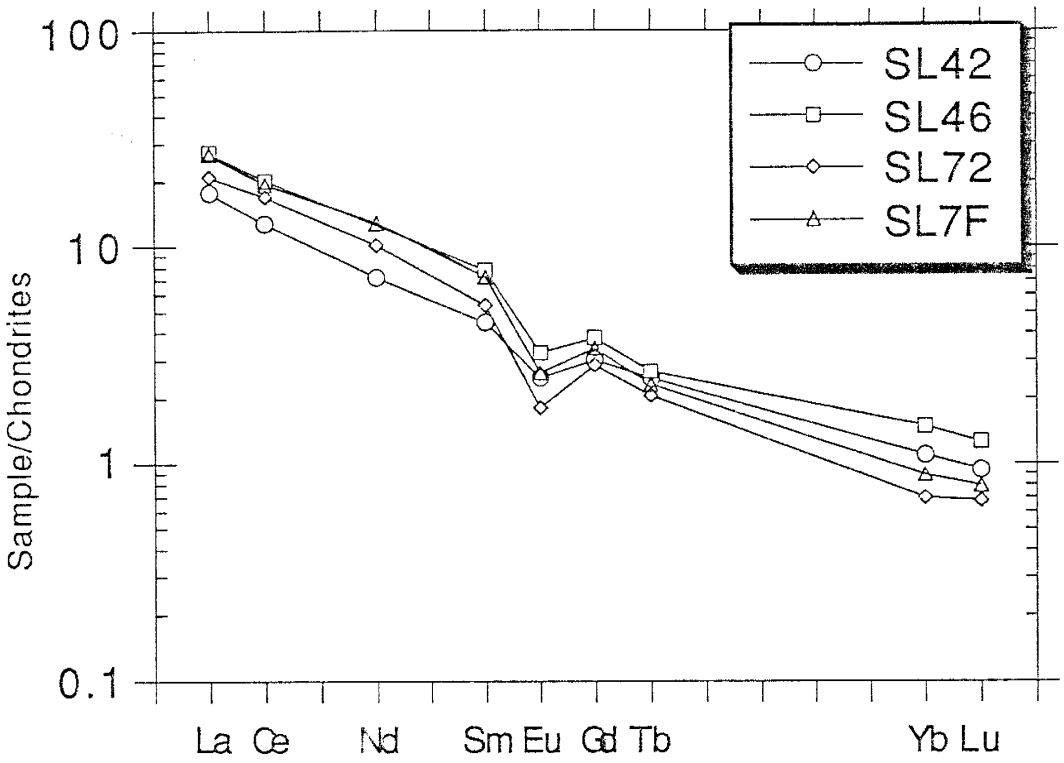

Figure 10b. Chondrite-normalized REE distributions for representative samples from the Sugarloaf Quartzite Formation. Chondrite values are from Haskin et al. (1968) and are given in Appendix C. Gd is estimated by $Gd_n = (Sm_n \times Tb_n^2)^{1/3}$.

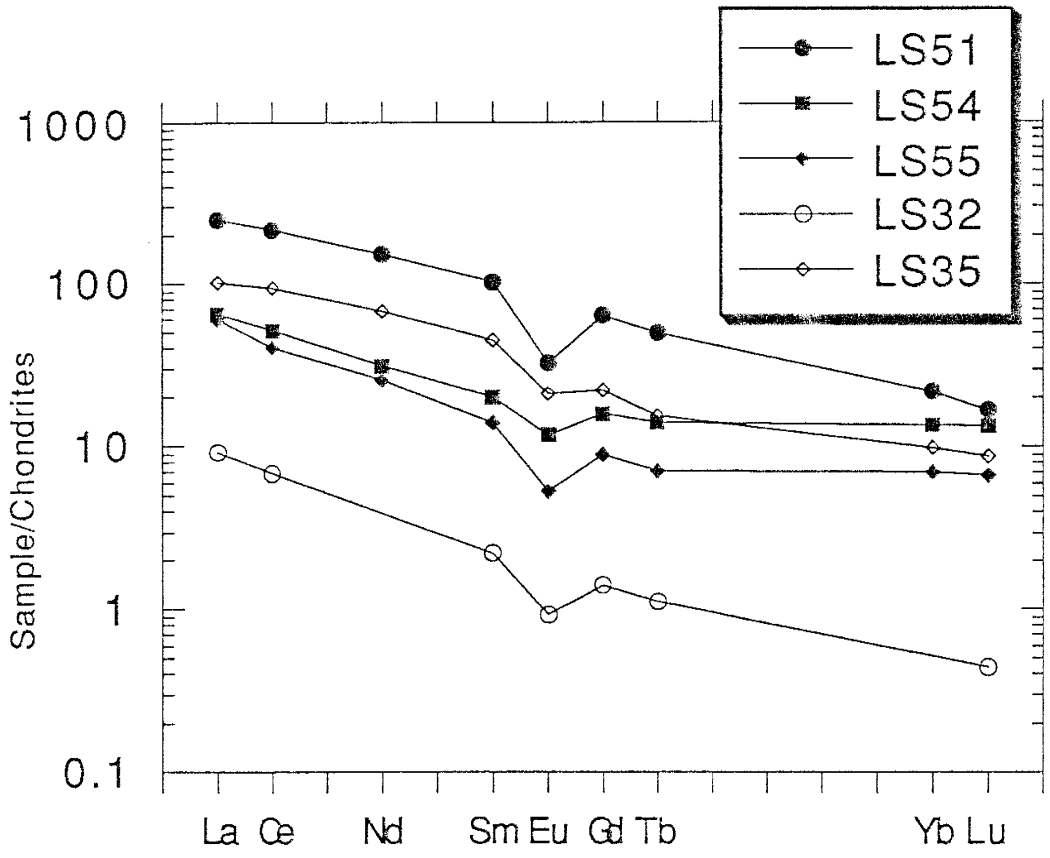

Figure 10c. Chondrite-normalized REE distributions of representative samples from the Lookout Schist. Pelites are shown with filled symbols while the quartzites have open symbols. Chondrite values are from Haskin et al. (1968) and are given in Appendix C. Gd is estimated by $Gd_n = (Sm_n \times Tb_n^2)^{1/3}$.

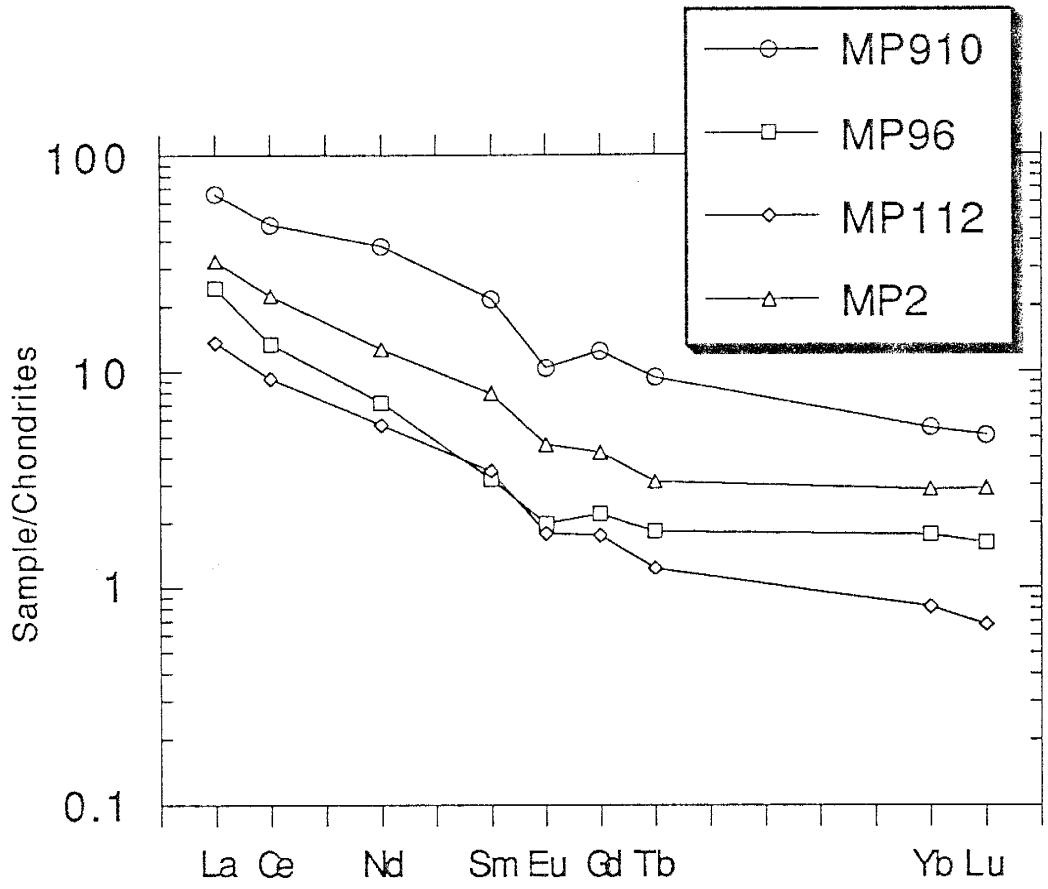

Figure 10d. Chondrite-normalized REE distributions for representative samples from the Medicine Peak Quartzite. Chondrite values are from Haskin et al. (1968) and are given in Appendix C. Gd is estimated by $Gd_n = (Sm_n \times Tb_n^2)^{1/3}$.

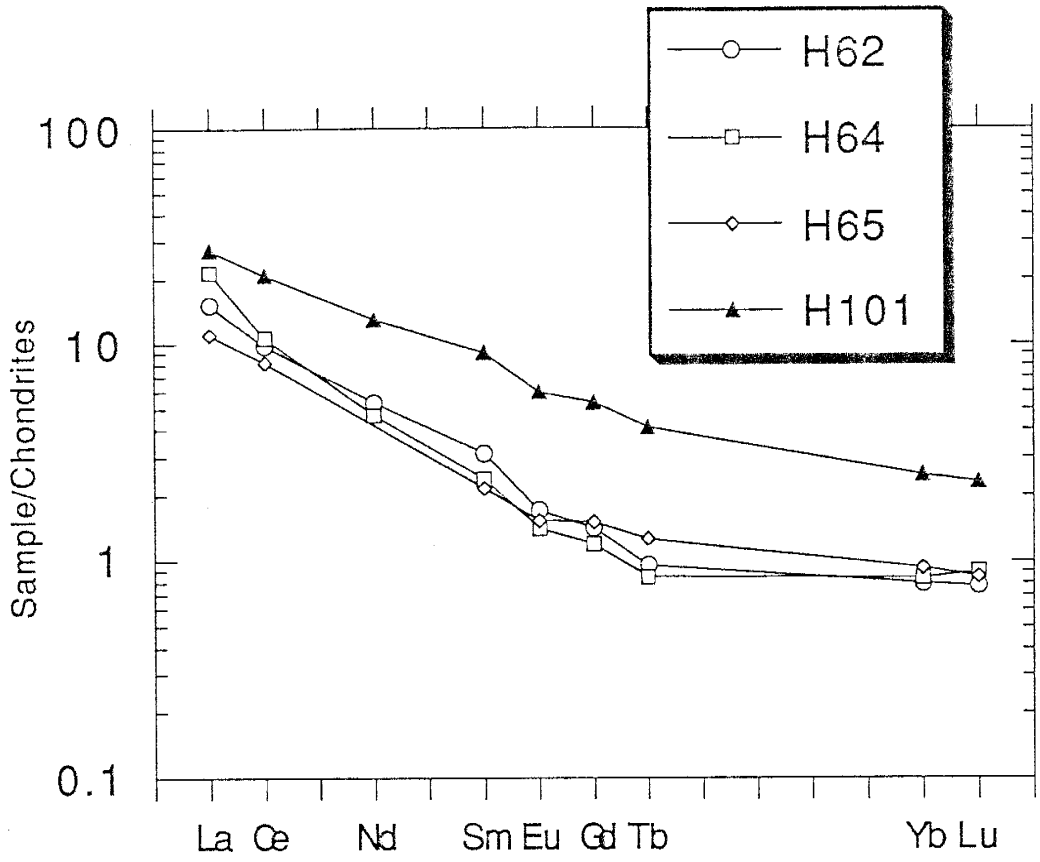

Figure 10e. Chondrite-normalized REE distributions for representative samples from the Heart Formation. The pelite is shown by the filled symbol while the quartzites have open symbols. Chondrite values are from Haskin et al. (1968) and are given in Appendix C. Gd is estimated by $Gd_n = (Sm_n \times Tb_n^2)^{1/3}$.

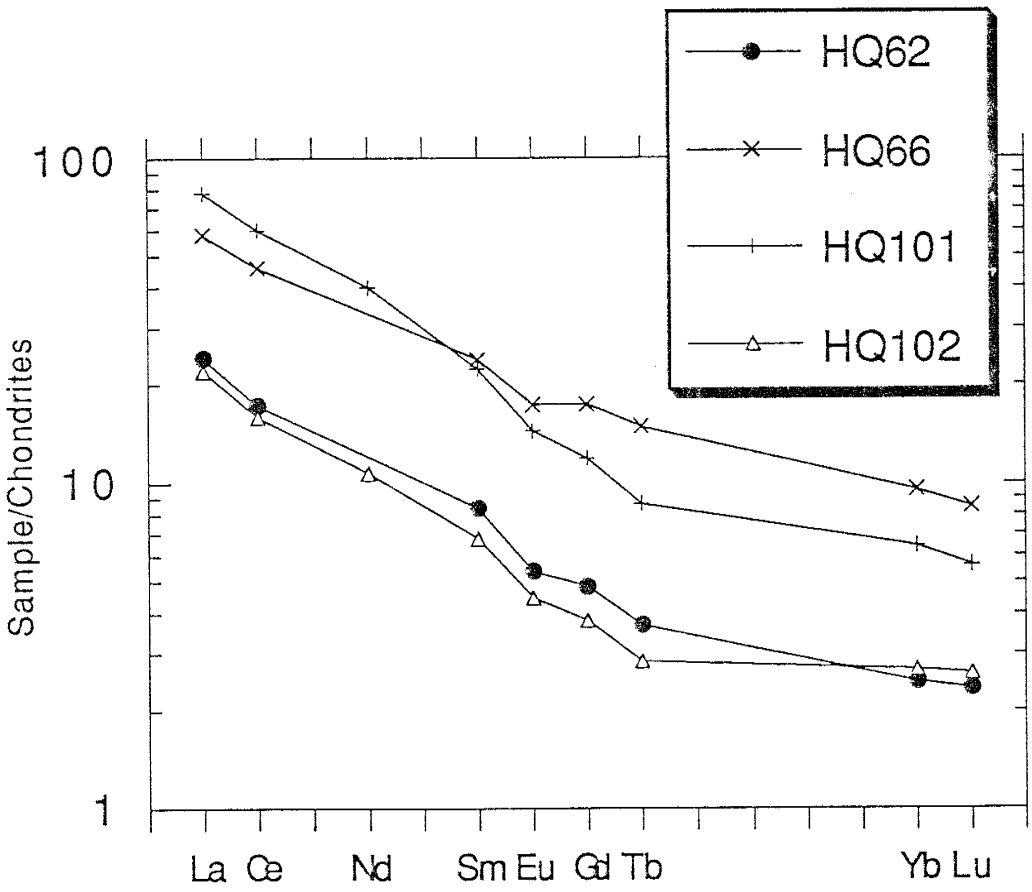

Figure 10f. Chondrite-normalized REE distributions of representative samples from the Headquarters Formation. The diamictites are shown by the + and x symbols while the pelite is shown by the filled symbol and the quartzite by the open symbol. Chondrite values are from Haskin et al. (1968) and are given in Appendix C. Gd is estimated by $Gd_n = (Sm_n \times Tb_n^2)^{1/3}$.

slopes of REE patterns for both quartzites and pelites suggests that the REE have similar mineralogical controls in both sediment types. It appears that the REE are controlled mainly by micas as is discussed later (in Mineral Separates section). Quartzites from the Medicine Peak and Sugarloaf Formations have more variable La_n/Yb_n ratios (11 to 49 and 16 to 30 respectively) than those from the Libby Creek pelites. This variability may be the result of analytical errors for Yb. Libby Creek quartzites typically contain ≤ 0.5 ppm Yb, which is close to the lower limit of detection by the INAA method used here.

Quartzites from the Headquarters, Heart, and Medicine Peak Formations show less Eu depletion than quartzites from the Lookout Schist, and Sugarloaf Formations. This is also observed in the pelites from these formations. In the Headquarters, Heart, and Medicine Peak Formations it is possible that detrital feldspar, which concentrates Eu but not other REE, is cancelling a larger original Eu depletion. However, calculations involving the effect of detrital feldspar on the size of the Eu/Eu* ratio indicate that an unreasonably large amount of feldspar is required to significantly change the size of the Eu anomaly in both pelites and quartzites (Fig. 11). For example, addition of 30% feldspar to PAAS will decrease the size of the negative Eu anomaly by only 4%, but addition of 30% feldspar to a quartzite will reduce the Eu anomaly by 20%. Since the amount of Eu depletion is similar for both pelites and quartzites from the Headquarters and Heart Formations, it appears that detrital feldspar has not significantly affected the Eu/Eu* ratio in the quartzites. Another line of evidence against the Eu/Eu* ratio being affected by concentration of feldspar is that pelites from the Lookout Schist have Na and Ca contents similar to

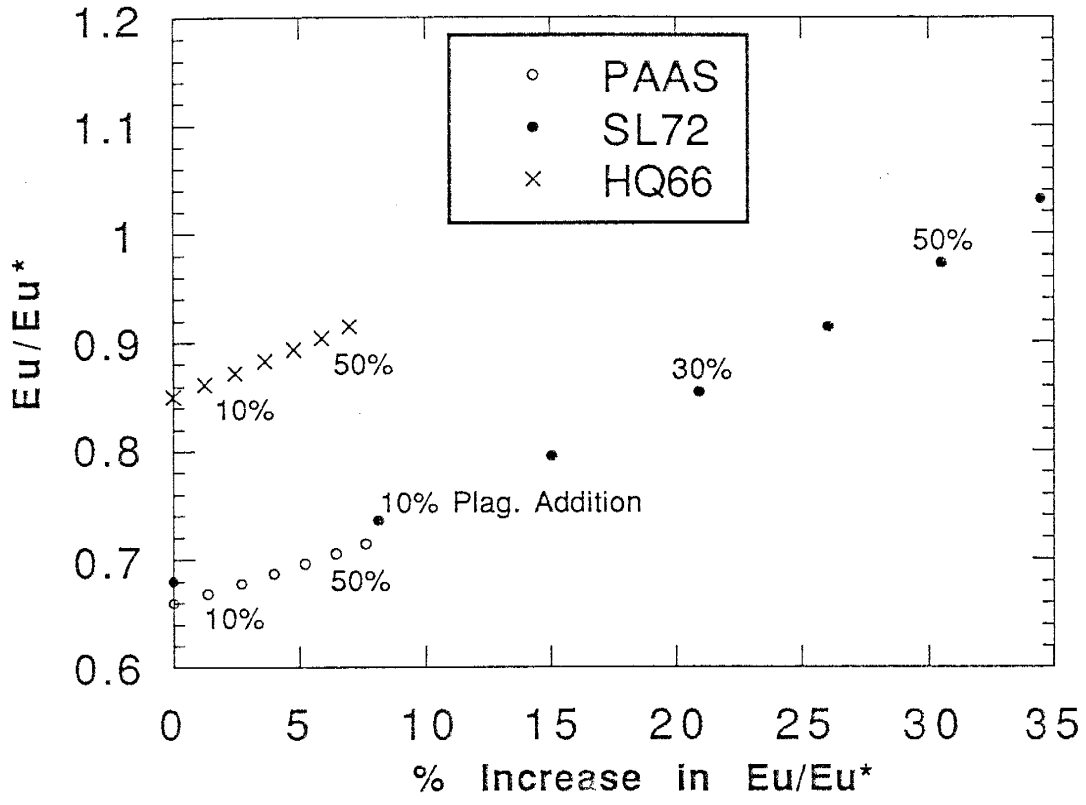

Figure 11. The effect of plagioclase addition (in 10% increments) on the size of the negative Eu anomaly (as measured by Eu/Eu*) in pelites and quartzites. PAAS (Post Archean Average Shale) (Taylor and McLennan, 1985) composition is given in Appendix C. Feldspar composition from Gromet and Silver (1983). Sample SL72 is a quartzite (Table B-2), and sample HQ66 is a diamictite (Table B-1). $Eu/Eu^* = Eu_n/(Sm_n \times Gd_n)^{1/2}$. Gd estimated by $Gd_n = (Sm_n \times Tb_n^2)^{1/3}$.

those from the Headquarters and Heart Formations, but have Eu/Eu* ratios typical of sediments from the upper Libby Creek Group.

A thin quartzite unit sampled at the base of the French Slate (FS15) has an unusual REE pattern (Fig. 10 a). Concentrations of the REE are very low, and the pattern is relatively unfractionated. The most striking feature is its large positive Eu anomaly, which is similar to those contained in hydrothermal fluids (Michard 1989). This sample consists of quartz, Fe-Ti oxides and minor carbonate. These minerals typically contain low concentrations of REE, but carbonate can accommodate a small amount of Eu in the +2 valence state. It is likely that this sample has been hydrothermally altered, as such it will be excluded from provenance discussions.

Mineral Separates

A medium-grained fuchsitic quartzite (MP1) was selected for mineral separation to better understand the mineralogical locations of trace elements in Libby Creek sediments and to evaluate these in terms of provenance. MP1 contains 83-85% quartz, 15-17% fuchsite and minor amounts of zircon, sphene, apatite and Fe-Ti oxides. The original detrital minerals probably consisted of quartz, clay minerals (now fuchsite), zircon, apatite and Fe-Ti oxides. It is possible that some primary phases have been completely removed through diagenetic or metamorphic processes. The detrital origin of zircon and apatite is indicated by their subrounded shapes. The textural relationships, in thin section, of sphene, fuchsite, and some Fe-Ti oxides suggests they are secondary minerals. The quartz in MP1 is recrystallized. Quartz, fuchsite, zircon and sphene are present in quantities large enough to be chemically analyzed. However, the

concentrations of trace elements in the quartz fraction are extremely low and do not significantly contribute to the trace element abundances of the whole rock.

The separated phases were analyzed by INAA (Table B-3). The REE distributions of the whole rock and fuchsite are similar, but the fuchsite contains about 4x the concentration of REE in the whole rock (Fig. 12). This suggests that the REE in the whole rock are controlled predominantly by fuchsite (originally clay minerals). The LREE are depleted relative to the HREE in zircon, but all are strongly enriched (200 to 1000x) relative to chondrites (Fig. 12) which is typical of zircon from felsic igneous rocks (Gromet and Silver, 1983; Heaman et al., 1990). The zircon from MP1 differs from other zircons in felsic rocks in that it has no negative Eu anomaly. Sphene has a relatively flat REE pattern but shows a weak negative Ce anomaly and a weak positive Eu anomaly (Fig. 12). REE concentrations in sphene from MP1 are approximately 20x chondrites while sphene from igneous rocks are typically 2000x chondrites (Gromet and Silver, 1983; Sawka, 1988). This may also indicate that the sphene is metamorphic in origin.

In order to understand which phases are most important in controlling Th, U, Hf, Ta, Sc, Cr, Co, and the REE, mass balances have been calculated (Fig. 13). The largest source of error in these calculations is arriving at accurate modal estimates of minerals, especially minor minerals. Fuchsite is estimated to make up approximately 17% of sample MP1. This estimate is based on thin section and chemical constraints. Since fuchsite is the only observed phase that contains Al, it is assumed that all the Al_2O_3 in the whole rock sample is contained in fuchsite. By using published Al_2O_3 contents of fuchsites, it is calculated that approximately 17% fuchsite

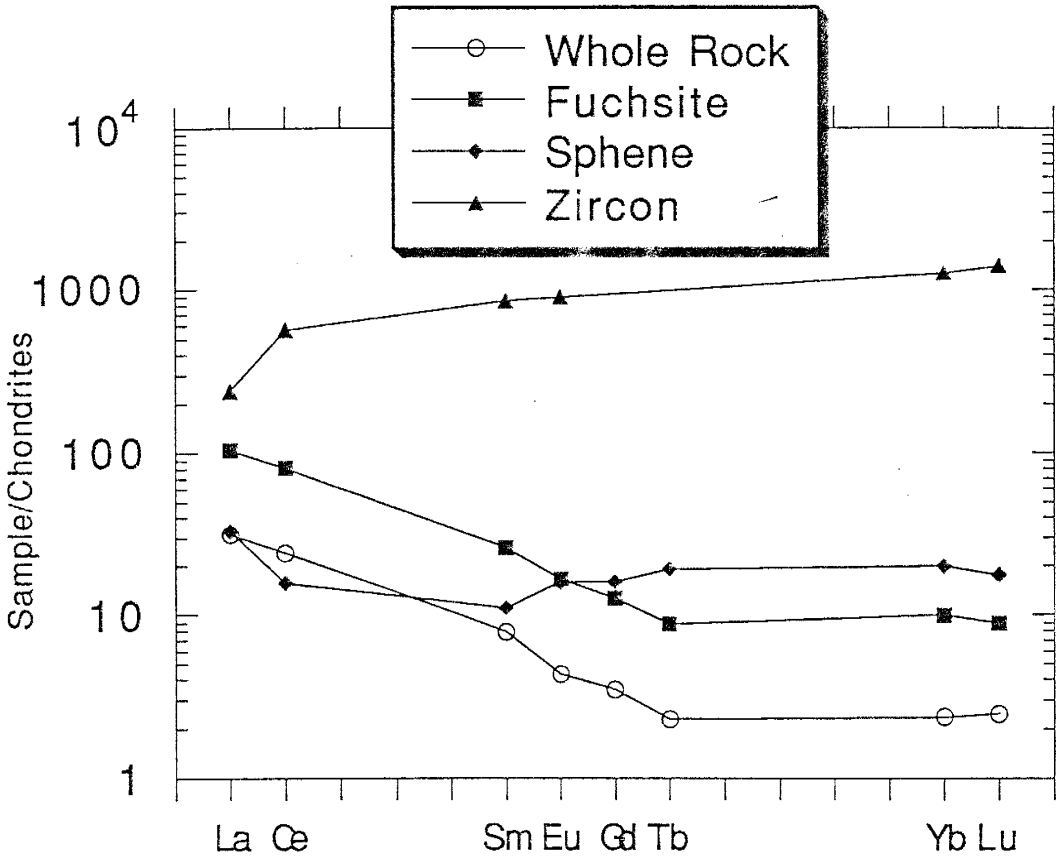

Figure 12. Chrondrite-normalized REE distributions for minerals separated from sample MP1 (Medicine Peak Quartzite). Whole-rock REE pattern is also shown. Chondrite values from Haskin et al. (1968) and are given in Appendix C. Gd estimated by $Gd_n = (Sm_n \times Tb_n^2)^{1/3}$.

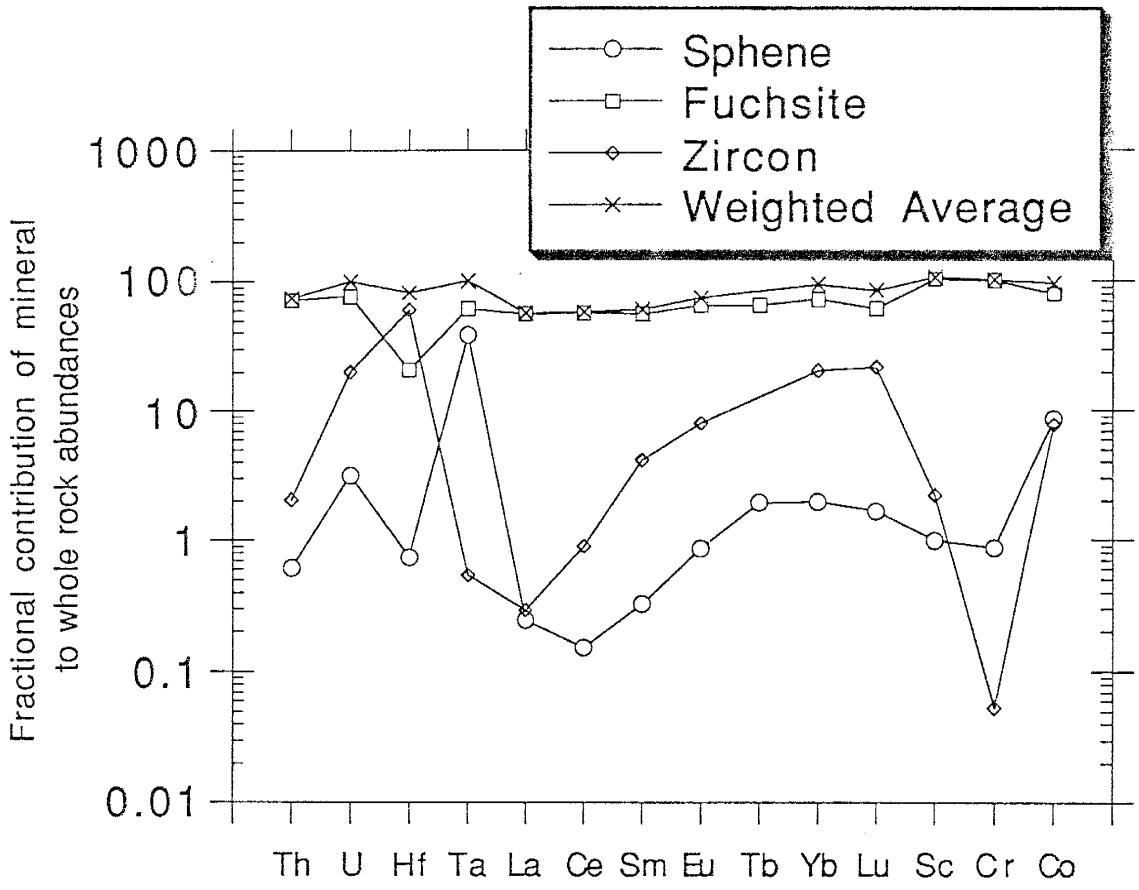

Figure 13. Fractional contribution of separated minerals to the trace element abundances in the whole-rock for sample MP1 (Medicine Peak Quartzite). A weighted average of these minerals is also shown. The composition of each mineral is given in Appendix B, Table B-3.

is contained in this sample which agrees well with thin section estimates. The amount of zircon present is estimated by assuming that all the zirconium present in the whole rock is contained in zircon, and that zircon contains approximately 50 weight percent zirconium. This results in approximately 0.04% zircon present in the whole rock. The least reliable estimate is for sphene. After correcting the whole-rock CaO for apatite (1.3 times the P_2O_5 content of the whole rock gives the amount of CaO needed to make apatite), it is assumed that the remaining CaO is contained in sphene. This gives 0.24% sphene in the sample, but this percentage is almost certainly an overestimation due to the possibility that some Ca is contained in the mica fraction (originally absorbed onto clay minerals) or other phases. Figure 13 shows the results of this mass balance calculation. It is observed that the major fraction of Th, U, REE, Sc, Co, Cr in this sample is contained in the fuchsite, which suggests that these elements were originally contained in clay minerals. Zircon controls only about 20% of the U and each of the HREE in the whole rock, but it does control 60% of the Hf (Fig. 13). Sphene controls 40% of the Ta present in the whole rock but less than 2% of the other trace elements (Fig. 13). Problems are encountered in accounting for the total mass of Th and the LREE. While fuchsite contains most of these elements, a significant fraction (30-40%) cannot be accounted for. It is possible that these elements are located in the phases not analyzed, Fe-Ti oxides and apatite. If all the P_2O_5 present in the whole rock is contained in apatite and all the Fe is in magnetite, only 0.01% apatite and 0.4% magnetite can be present. Using published compositions of these phases (Gromet and Silver, 1983; Cullers et al., 1987) it is concluded that they will not significantly affect the mass balance calculations (total of both phases, LREE 3%, HREE 4%). The most likely explanation is that an

unobserved phase or phases, which is enriched in Th and the LREE, is present in MP1. This phase(s) is either present in such low abundances or is too fine-grained to have been noticed. A possible minor phase is monazite, which is known to concentrate both the LREE and Th and is known to be stable in sedimentary and diagenetic environments. Using the average composition of monazites published by Lee and Bastron (1967) and inverting the mass balance calculation, it is found that only 0.0044% monazite is needed to account for the missing fraction of the LREE and Th. The addition of this amount of monazite will not affect the HREE mass balance significantly (<5% for each).

It has been shown that the REE distributions in MP1 are controlled mainly by the micas, although zircon and monazite can alter these distributions. In order to extrapolate these results to the other sediments from the Libby Creek Group, the effects of monazite and zircon on the REE distributions needs to be evaluated for each sample.

The effects of concentrating detrital monazite are difficult to evaluate. However, if monazite is the main control of Th and the LREE, good correlations should exist between these elements, but not between Th and HREE. However, a positive correlation exists between Th and the HREE, suggesting that monazite is not an important phase in controlling REE in these sediments.

In order to evaluate the effect of zircon on the HREE distributions of all samples, an upper limit of the amount of zircon contained in each sample has been calculated by assuming that all the Zr present in the sample is contained in zircon. By using the Yb content of the zircons from MP1, the fraction of Yb in the sample controlled by zircon is calculated (Fig. 14). Less than 5% of the Yb for most of the Libby Creek pelites is contained in zircon,

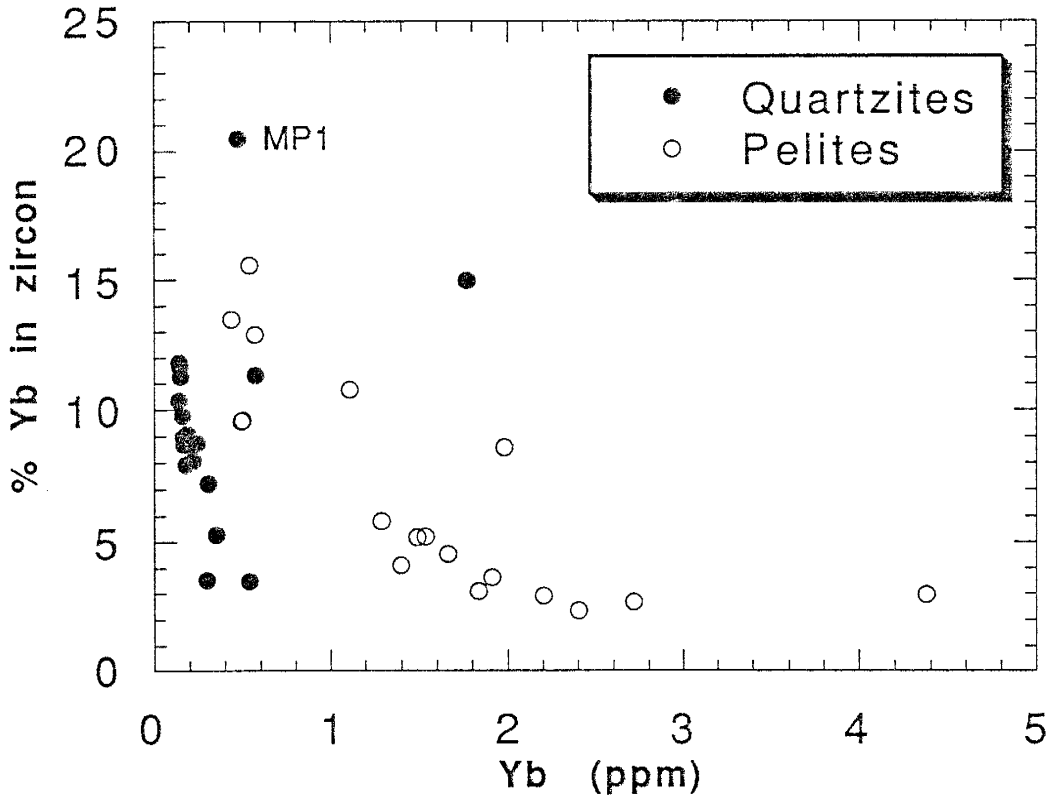

Figure 14. Percent Yb controlled by zircon versus Yb in the whole-rock sample for quartzites and pelites from the Libby Creek Group. All the Zr contained in the whole-rock is assumed to be contained in zircon, and zircon is assumed to contain 250 ppm Yb (the composition of zircon analyzed in this study).

while for the quartzites and some quartz-rich pelites up to 20% of the Yb is contained in zircon. It is concluded that zircon is not important in controlling the HREE distributions of the Libby Creek sediments. Similar conclusions were reached for shales by Condie (1991) and McLennan (1989) and for Tertiary sandstones by Miliken and Mack (1990).

DISCUSSION

Paleoweathering

Elements that are progressively lost during weathering of fresh rocks are useful in understanding climatic conditions in the sources of fine-grained clastic sediments. The most useful elements for this purpose are Na, Ca and Sr (Nesbitt et al., 1980; Harnois, 1988). The amount of each of these elements remaining in the soils developed on fresh rock is related to the intensity of chemical weathering under which the soils formed. Many chemical weathering indices have been developed, (Nesbitt and Young, 1982; Harnois, 1988; Chittleborough, 1991) but in this study only the CIW (chemical index of weathering) is considered. The CIW exploits the fact that Na and Ca are mobile during weathering, while Al is immobile under most weathering conditions. It is defined as $(Al_2O_3/(Al_2O_3 + Na_2O + CaO))$ x 100 with Al, Na and Ca in molar proportions (Harnois, 1988). While the CIW accurately records the degree of chemical weathering in soil profiles, its use in sediments is complicated by topographic relief. Relief and climate can work against each other in that high relief may remove soils that are chemically only partially in climatic equilibrium (Pettijohn et al., 1973). However, calculation of chemical weathering indices for modern shales deposited under various climatic conditions indicates that they correlate reasonably well with climate (McLennan et al., 1990; Maynard et al., 1991). In shales, the more intense the chemical weathering of the source rocks, the higher the CIW value. For comparison purposes, PAAS has a value of 81 while fresh igneous rocks range between 40 and 60.

The CIW ratio indicates that extreme climatic variations occurred between the deposition of the Headquarters and French Slate formations.

Pelites from the Headquarters and Heart Formations have low CIW values ranging between 50 to 67 (Fig. 15). The low CIW values indicate that the intensity of chemical weathering for the source rocks of the Headquarters and Heart Formations was relatively low, supporting a glacial depositional environment for the Headquarters Formation. Pelites from the French Slate have much higher CIW values (85 to 93). These high values indicate a large degree of chemical weathering affected the French Slate source rocks. Similar CIW values are obtained from weathering profiles developed in tropical regions (Harnois, 1988; Marsh, 1991). Pelites from the Lookout Schist have highly variable CIW values (46 to 85). The Lookout Schist is arkosic in places, therefore the large range in CIW values likely reflects variable concentration of plagioclase and not paleoweathering conditions.

The use of the CIW in quartzites can also be complicated by the possibility of hydraulic concentration of plagioclase in sands. CIW values are highly variable for some Libby Creek quartzites, but for other formations, CIW values are in agreement with those obtained from associated pelites. Quartzites from the Headquarters and Heart Formations show a large range in CIW values (40 to 82), with a much larger spread than is observed for the pelites from these formations (Fig. 15). The CIW values of quartzites from the Medicine Peak Formation range from 65 to 89, and these values are intermediate between pelites from the Headquarters Formation and the French Slate. The Sugarloaf Quartzite also shows intermediate CIW values ranging from 58 to 70. Although the CIW values from the Medicine Peak and Sugarloaf Quartzites seem to make sense in terms of the pelite data, the significance of these values is unknown. The mobile nature of Na and Ca and the high permeability of sandstones also opens the possibility that diagenetic or metamorhpic fluids

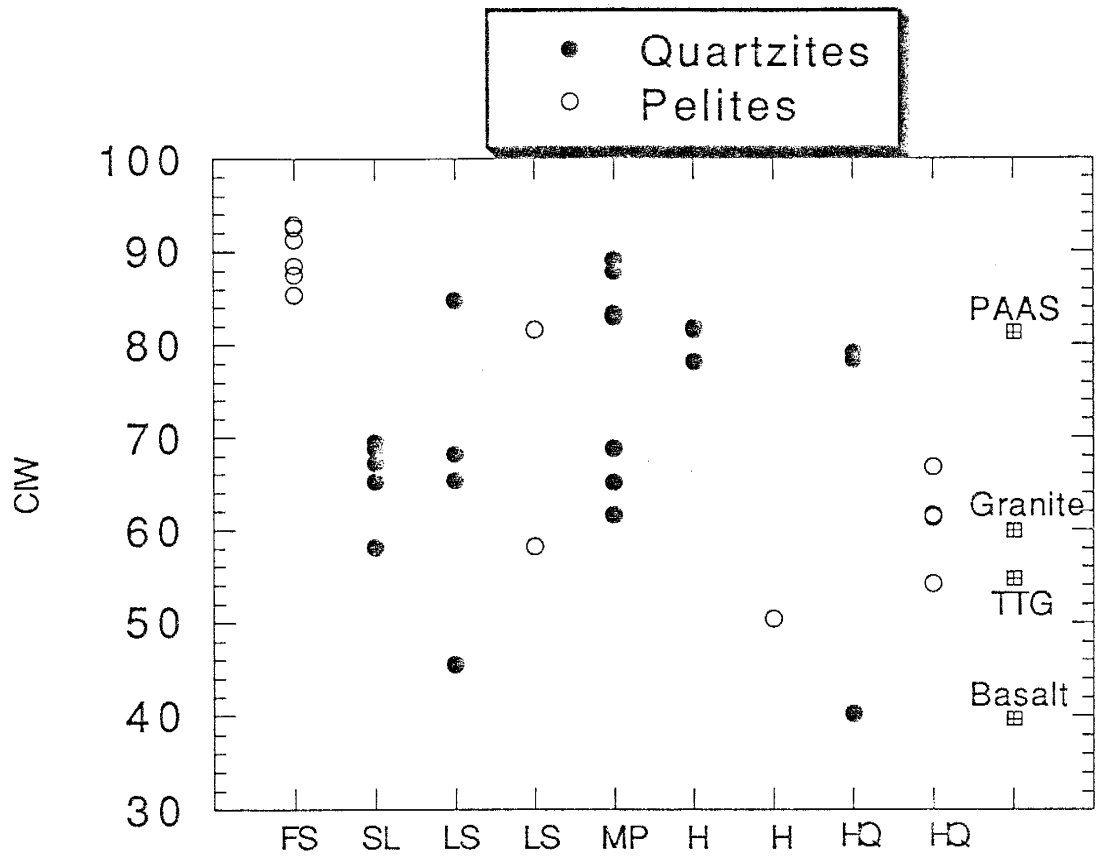

Figure 15. CIW versus stratigraphic height for clastic sediments from the Libby Creek Group. FS = French Slate, SL = Sugarloaf Quartzite, LS = Lookout Schist, MP = Medicine Peak Quartzite, H = Heart Formation, HQ = Headquarters Formation. Shown for comparison are Archean Granite, Basalt, TTG (Archean averages from Condie (1992)) and PAAS (Post Archean Average Shale (Taylor and McLennan, 1985)). Compositions for these rock types are given in Appendix C.

may have contributed to the present CIW values observed in the quartzites. Therefore, interpretations of paleoclimatic conditions, using chemical weathering indices, from quartzites is tenuous at best.

The behavior of many elements during high degrees of chemical weathering is complex and not fully understood. The strong positive correlations between the CIW and K, Rb and Cs in the French Slate supports the idea that these elements are fixed onto clays during chemical weathering (Nesbitt et al., 1980). Other strong positive correlations in the French Slate occur between the CIW and Cr/Th ($r = 0.96$), Eu/Eu* ($r = 0.95$), La_n/Yb_n ($r = 0.90$) and Gd_n/Yb_n ($r = 0.88$). Although fractionation of REE under extreme weathering conditions in soil profiles is not unusual (Loubet and Allegre, 1977; Duddy, 1980; Schau and Henderson, 1983; Nesbitt et al., 1990), it is assumed that the REE are homogenized as a result of thorough mixing during transportation and deposition (Taylor and McLennan, 1983). The physical meaning of these correlations is unknown at present.

The progressive loss of Sr in weathering profiles is also a good indicator of paleoweathering (Nesbitt et al., 1980). As discussed above, sediments from the Medicine Peak Quartzite, Lookout Schist, Sugarloaf Quartzite, and French Slate show significant Sr depletion relative to PAAS while sediments from the Headquarters and Heart Formations show little or no Sr depletion (Figs. 7, 8). Depletion is greatest in the Lookout Schist and French Slate while the Medicine Peak Quartzite shows depletion intermediate between the French Slate and Headquarters Formation possibly indicating a gradually changing climate. The Sr data supports the climatic results inferred from the CIW.

Other evidence of paleoclimatic conditions comes from the unusual suite of aluminosilicate minerals (sericite, pyrophyllite, and kyanite) in the

Medicine Peak Quartzite. Kaolinite is also present, but it is likely a product of modern weathering. Young (1973) has suggested these minerals result from extreme chemical weathering of source rocks while Karlstrom et al. (1983) have interpreted these minerals to be products of in-situ alteration of feldspars during diagenesis or metamorphism. Similar aluminosilicate mineral assemblages are found in the extensive Mid-Proterozoic quartzites of the Mid-Continent region. Dott (1983) has effectively demonstrated that these minerals likely form in warm, humid climates coupled with low relief. The CIW values and degree of Sr depletion could be used to support a similar origin for these minerals in the Medicine Peak Quartzite.

Quartzites as Provenance Indicators

The use of quartzite chemistry in provenance studies has always been approached with caution (Taylor and McLennan, 1985; Cullers, 1988; Cullers et al., 1988). Hydraulic sorting of minerals and diagenetic processes (especially intrastratal solution) can erase much of their provenance memory. During diagenesis zircon, apatite, monazite, chromite and Ti-oxides are relatively stable, whereas garnet, pyroxene, amphibole and Fe-oxides are highly susceptible to dissolution (Milliken and Mack, 1990; Milliken, 1988; Pettijohn, 1941). The loss of these minerals can have significant consequences on the trace-element distributions in quartzites. Shales, on the other hand, appear to be relatively unaffected by intrastratal solution because of their low permeability, although some studies indicate that some shales have been affected (Blatt, 1985).

Quartzites from the Libby Creek Group have REE distributions similar to associated pelites. Abundances are lower, but the slopes on chondrite-normalized REE plots and important ratios such as Eu/Eu* and La_n/Yb_n

are similar, although these ratios are more variable in the quartzites than in the pelites. The similarity of REE distributions and the mineral separate data discussed above suggests that mica (originally clay minerals) is the controlling phase for REE in both quartzites and pelites. The REE distributions in the quartzites appear to reflect those of their source rocks. However, due to the low abundances of the REE in the quartzites, REE-enriched minor phases such as zircon and monazite can significantly affect REE distributions. However, this is not observed for the Libby Creek sediments.

Ratios commonly used as provenance indicators in shales (La/Sc, Th/Sc, Cr/Th, Ba/Co, Zr/Y and Zr/Cr) are highly variable in the Libby Creek quartzites, even within the same formation (Figs. 16a-b). Figure 16a demonstrates the greater variability of the Th/Sc ratio with increasing SiO_2 content. Most of the variation in these ratios, except in the Zr/Y ratio, is controlled by the low concentrations of Sc, Cr, Ni, and Co in the quartzites. A likely explanation for the low concentrations of the transition metals in the quartzites is that Fe-Ti oxides, which are enriched in these elements, are rare in the quartzites. It is possible that loss of the Fe-oxides through intrastratal solution has also depleted the quartzites in Sc, Cr, Ni, and Co. Supporting this view in the quartzites are positive correlations between these metals and Al, suggesting that the metals are contained mainly in the micas. This conclusion is also supported by the mineral separate data. The good correlations between metals and Al in the quartzites could result from the removal of other phases that control these metals, such as Fe-Ti oxides. Such element correlations in the pelites, however, are poor, suggesting more than one controlling phase for these metals in shales.

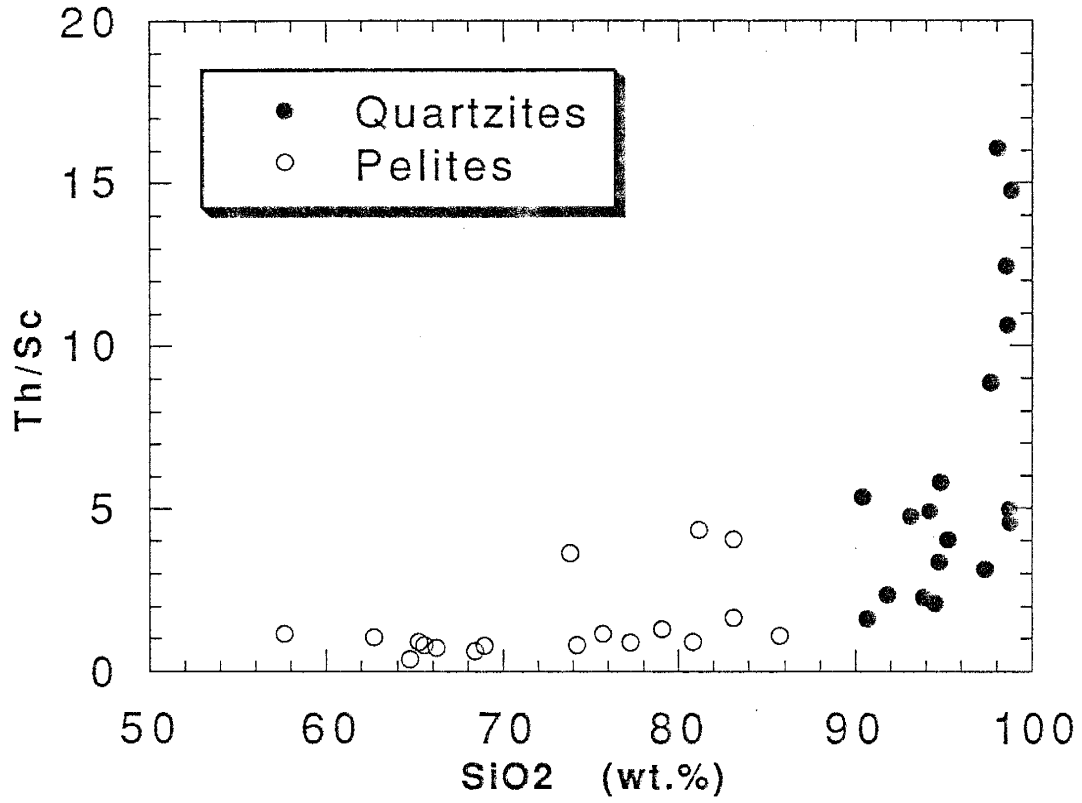

Figure 16a. Th/Sc versus SiO_2 diagram for quartzites and pelites from the Libby Creek Group.

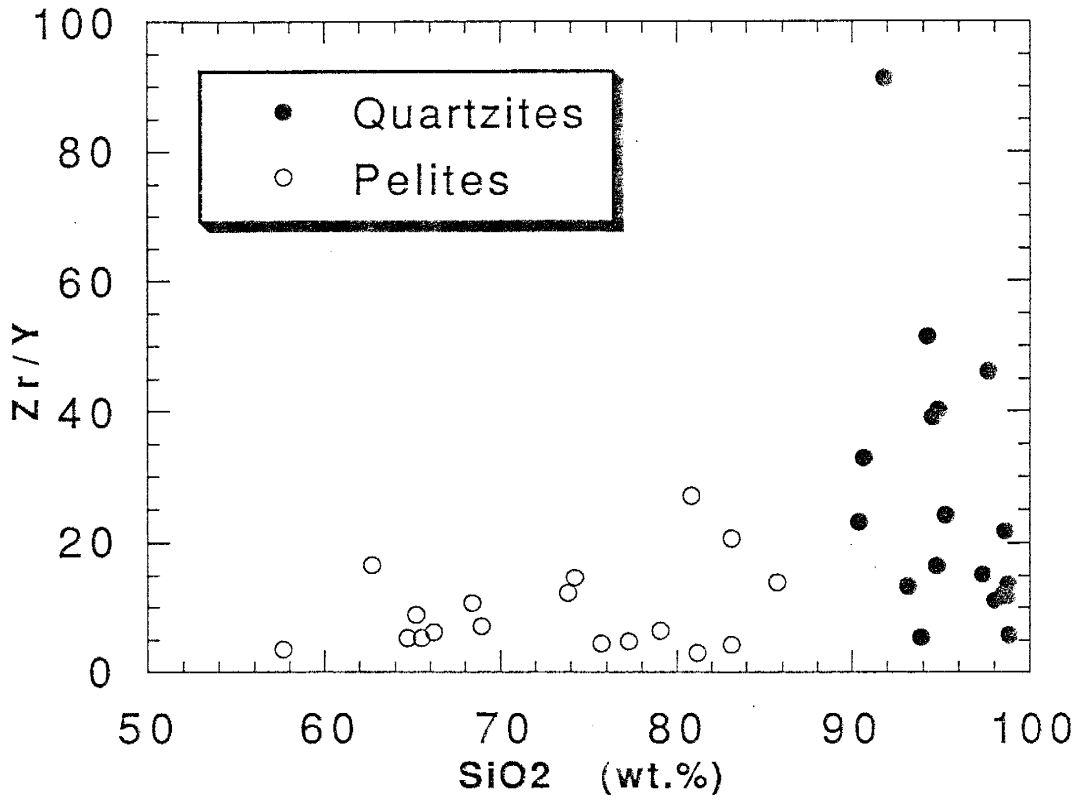

Figure 16b. Zr/Y versus SiO_2 diagram for the quartzites and pelites from the Libby Creek Group.

Another possibility for the lack of Fe-Ti oxides in Libby Creek quartzites is that these minerals were very fine-grained in the source rocks, and therefore followed clay minerals during transportation and deposition. However, Blatt and Sutherland (1969) demonstrated that the grain size of heavy minerals in sand-shale pairs of Tertiary sediments are identical. Although shales have a smaller fraction of heavy minerals than sands, the heavy mineral population in the shales is more diverse.

Ratios such as Zr/Y and Zr/Cr can also be affected by hydraulic concentration of zircon in the quartzites. Figure 16b demonstrates the greater variability of the Zr/Y ratio with increasing SiO_2 content. Shales typically have Zr contents of 200 ± 100 ppm while quartzites from the Libby Creek Group have Zr contents ranging from 30 to 550 ppm, reflecting the highly variable concentration of zircon. Therefore, the Zr/Cr and the Zr/Y ratios in the quartzites may not reflect these ratios in the source rocks and must be used with caution.

Provenance and Tectonic Implications

REE distributions indicate a change in source-area composition occurred between the deposition of the Medicine Peak Quartzite and the Lookout Schist. An abrupt change in the size of the negative Eu anomaly occurs between these two formations (Fig. 17). The sudden increase in size of the negative Eu anomaly may reflect the addition of K-rich granites, which are commonly Eu depleted, to the source area. K-rich granites are widespread in the Late Archean of the Wyoming Province (Peterman and Hildreth, 1978; Stuckless et al., 1985) and in other Late Archean terrains worldwide (Taylor and McLennan, 1985), but are relatively minor components of Early Archean terranes. The rapid change in the size of the Eu/Eu* ratio in the

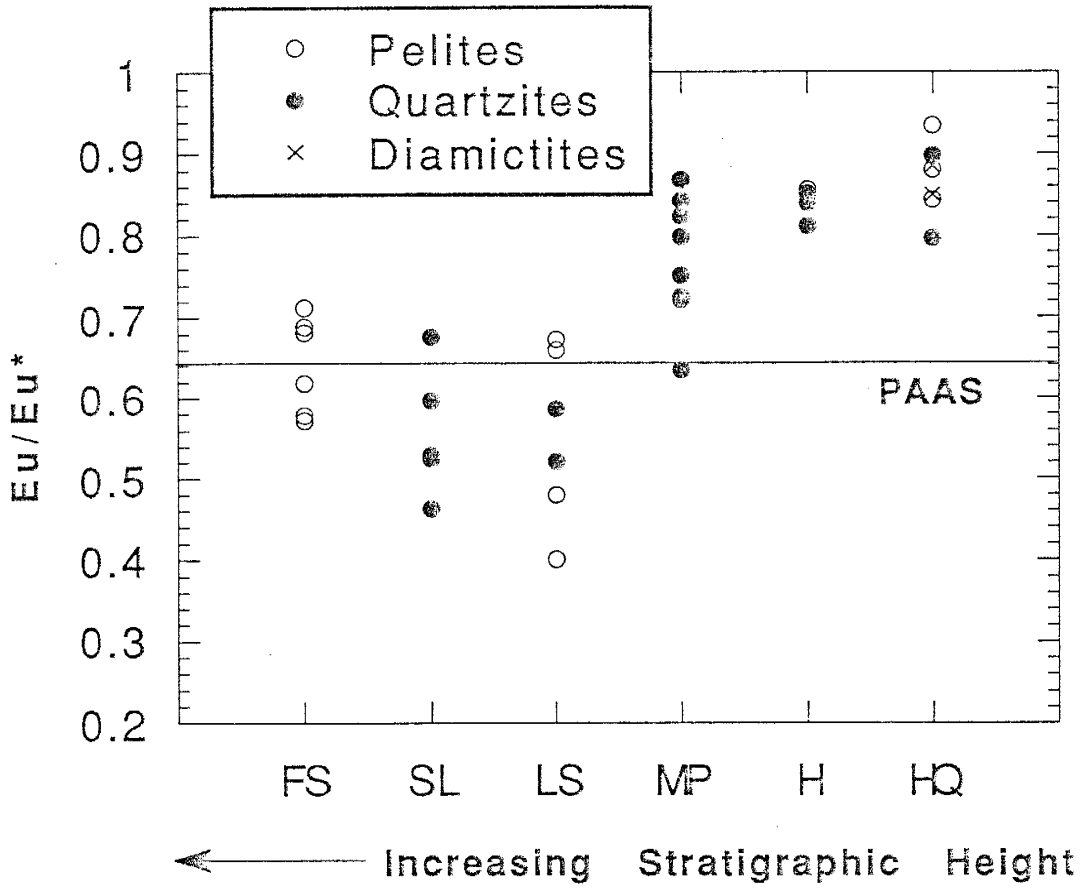

Figure 17. Change in the size of the negative Eu anomaly, as measured by Eu/Eu*, with stratigraphic height. FS = French Slate, SL = Sugarloaf Quartzite, LS = Lookout Schist, MP = Medicine Peak Quartzite, H = Heart Formation, HQ = Headquarters Formation. The Eu/Eu* ratio for PAAS (Taylor and McLennan, 1985) is shown for comparison. $Eu/Eu^* = Eu_n/(Sm_n \times Gd_n)^{1/2}$. Gd estimated by $Gd_n = (Sm_n \times Tb_n^2)^{1/3}$.

Libby Creek sediments likely indicates intrusion of Eu depleted granite into and uplift of the source regions. Without uplift, the Eu/Eu* ratio should gradually decrease with time as erosion progressively unroofed K-rich granites. Instead, a sharp break in the size of the Eu/Eu* ratio occurs (Fig. 17). The size of the negative Eu anomaly and other trace element distributions in the French Slate is typical of Phanerozoic shales possibly indicating stabilization of the Wyoming Province by the time of its deposition. Karlstrom et al. (1983) suggested that the French Slate may in part represent detritus from approaching Proterozoic island-arc terranes from the south. However, the French Slate shows none of the trace-element distributions that are typical of arc sediments. A recently published Nd model age study on the Libby Creek sediments shows that Nd model ages do not change significantly with stratigraphic height, and that only detritus from the Archean Wyoming Province is required to explain the observed model ages (Ball and Farmer, 1991).

Other geochemical indications of a change in source-area composition between the deposition of the upper and lower Libby Creek Group are observed in the fine-grained sediments. Sediments from the lower Libby Creek group have higher Sc, Cr, Co, Ni, Mg and Fe contents and lower Th, U, REE (except Eu), Ti and Nb contents than sediments from the upper Libby Creek Group. These trends suggest that the source area of the lower Libby Creek Group was more mafic in composition than that of the upper Libby Creek Group. Similar geochemical trends have been reported for other Early Proterozoic basins (Taylor and McLennan, 1983; 1985).

Elements that are extremely useful in modelling source-area composition of fine-grained sediments include REE, Th, Sc, and Co (Taylor and McLennan, 1985; Wronkiewicz and Condie, 1990). These elements are

thought to be transported virtually quantitatively from source rocks to sediments (Taylor and McLennan, 1985). Elements such as Cr and Ni are enriched onto clay minerals during source-area weathering (Condie and Wronkiewicz, 1990; Marsh, 1991), enhancing differences between the types of source rocks, but limiting their use in modelling. The HFSE (Ta, Nb, Zr and Hf) are mainly contained in heavy minerals and therefore, their concentrations in sediments are controlled mainly by hydraulic sorting of grains during transportation. The alkali and alkaline-earth metal distributions are strongly affected by source-area weathering and other secondary processes. Therefore, the concentrations of these elements in sediments probably do not reflect their concentrations in the source rocks. Although the REE, Th and possibly some HFSE may be unaffected by secondary processes in the quartzites, quartz dilution effects prevent their use in mixing models. However, ratios of these elements can be compared to ratios obtained after mixing of endmember compositions in varying proportions. Quartz dilution effects are negligible for pelites or diamictites since their SiO_2 and Al_2O_3 contents are similar to those of igneous rocks. Consequently, they can be used in mixing calculations.

Mass balance mixing equations were constructed for average compositions of fine-grained sediments from the upper and lower Libby Creek Group by using average compositions of the most common rock types of Archean terranes. Endmembers used are granite, basalt and TTG. The compositions used in the mixing calculations are given in Appendix C. Although komatiite is present in most Archean terranes, preliminary mixing calculations showed that only 2% could be present in the Libby Creek sediment source area, and that komatiite is not needed to explain any

of the observed element distributions. For this reason komatiite is not used in the mixing calculations.

Mixing is performed in a forward manner by continuously varying the amount of each endmember until satisfactory agreement between the sediment composition and the calculated composition is reached. Various methods for solving three variable mixing equations were tried, such as iteration techniques and least squares solution of simultaneous equations, but these methods often gave geologically unrealistic results (such as negative mixing proportions of endmembers). Problems with using mixing calculations to infer provenance include: 1) Choosing average compositions of endmembers, since actual source-rock compositions are not known. 2) The geochemical behavior of the elements used in modelling, in terms of weathering, transportation, diagenesis and metamorphism, are not fully understood. 3) Recycling of sedimentary rocks in the source area.

Mixing results show that sediments of the lower Libby Creek Group contain more TTG and basalt and less granite relative to sediments from the upper Libby Creek Group. A mixture of 40% TTG, 20% granite and 40% basalt agrees well with the composition of the lower Libby Creek Group, while a 25% TTG, 50% granite and 25% basalt mix agrees well with the composition of sediments from the upper Libby Creek Group. The agreement between REE distributions in upper Libby Creek sediments with those calculated from a 25:50:25 mix is excellent (Fig. 18). Both the concentrations and the slopes are virtually identical for these REE patterns. The lower Libby Creek sediments are compared to a 40:20:40 mix (Fig. 19). The slopes of these patterns are identical, but the abundances of the middle REE differ by up to 11%. Th, Sc, and Co are also in good agreement ($< 10\%$)

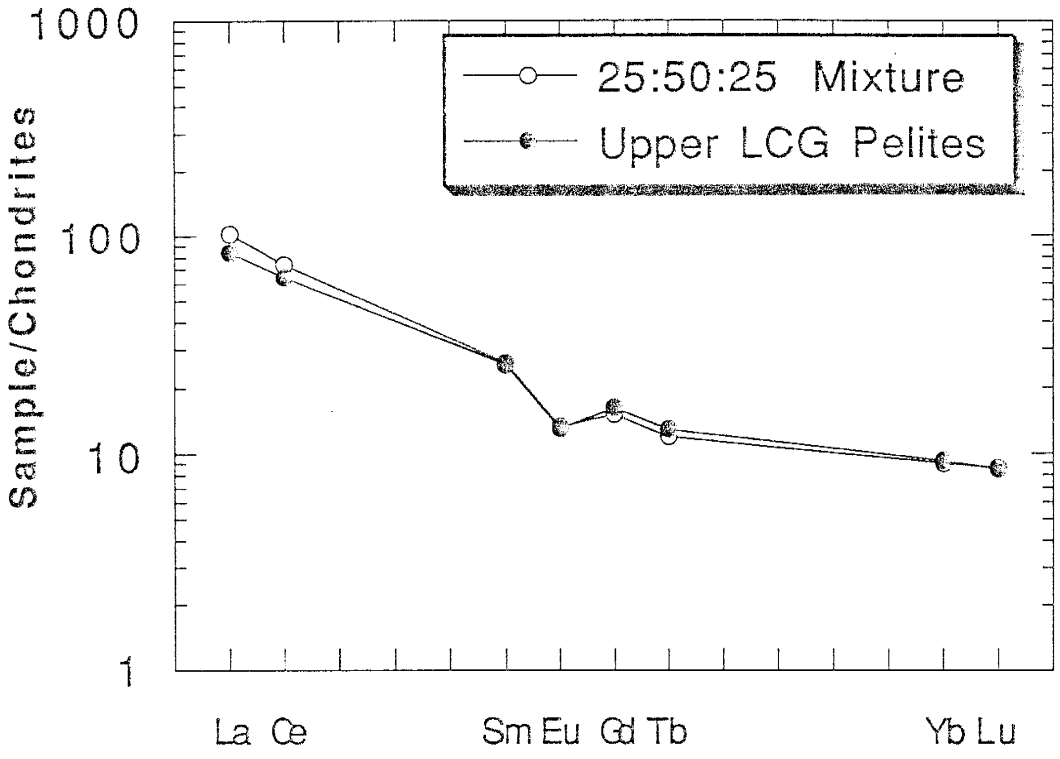

Figure 18. Chondrite-normalized REE distributions for an average pelite from the upper Libby Creek Group and calculated composition of the same pelite. Calculated pelite represents a mix of 25% Archean TTG, 50% Archean granite, and 25% Archean basalt. Composition of rock types used in mixing calculations are given in Appendix C and were compiled by Condie (1992). Chondrite values are from Haskin et al. (1968) and are also given in Appendix C.

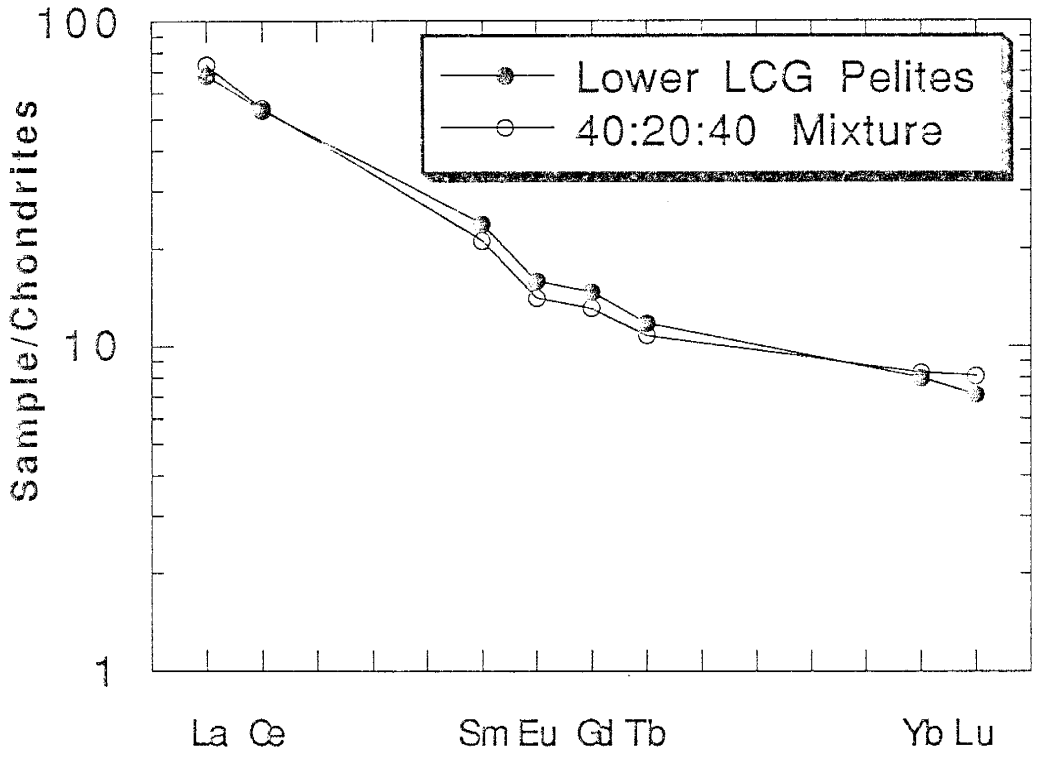

Figure 19. Chondrite-normalized REE distributions for an average pelite from the lower Libby Creek Group and calculated composition of the same pelite. Calculated pelite represents a mix of 40% Archean TTG, 20% Archean granite, and 40% Archean basalt. Composition of rock types used in mixing calculations are given in Appendix C and were compiled by Condie (1992). Chondrite values are from Haskin et al. (1968) and are also given in Appendix C.

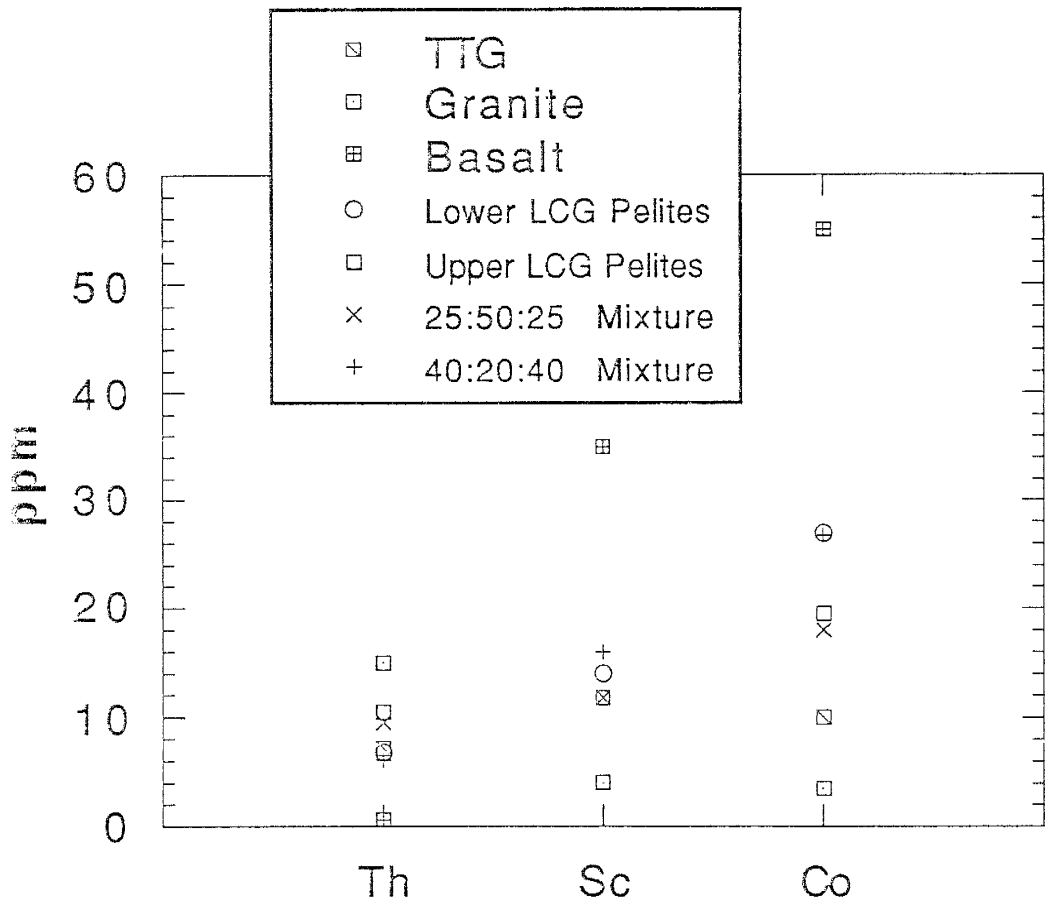

Figure 20. Comparison of pelite averages from the lower and upper Libby Creek Group and calculated compositions of the same pelites. Lower Libby Creek Group pelites are calculated from a 40:20:40 mix of Archean TTG:Granite:Basalt while the upper Libby Creek Group pelites are calculated from a 25:50:25 mix. Composition of rock types used in mixing calculations are given in Appendix C and were compiled by Condie (1992).

between the mixes and the sediment compositions of the upper and lower Libby Creek Group (Fig. 20). The usefulness of these calculations is clearly demonstrated. Not only is insight gained as to what rocks are present in the source area, but also what proportions these rocks occur in. Many assumptions go into these calculations, and it should be emphasized that the above solutions are not unique, although they agree well with the available data.

Standard petrographic and sedimentological methods are not sensitive enough to detect a change in source area composition between the deposition of the Medicine Peak Quartzite and the Lookout Schist and consequently went unreported by Karlstom et al. (1983).

Composition of the Late Archean Crust in the Wyoming Province

Understanding how the composition of the upper continental crust has changed through time is essential for understanding the evolution of the earth and its geodynamical processes. Many different approaches have been used to arrive at an average upper crustal composition. Typical methods involve large scale sampling of the exposed upper crust (Eade and Fahrig, 1973; Shaw et al., 1976) or various map scaling techniques (Condie, 1992). These methods may or may not yield reasonable upper crustal estimates due to sampling problems involved (i.e. the rocks exposed today may not be exposed in their original proportions or the exposed rock area may not be representative of their volume). An approach advocated by Taylor and McLennan (1985) uses the composition of fine-grained sediments. They assume that fine-grained sediments represent a homogeneous mixture of the exposed upper crust. In sediments, the abundances of relatively insoluble elements, such as REE, Th, Sc, and Co,

are thought to represent their mean abundance in the upper crust. Using sediments to arrive at the composition of the upper crust has the advantage that we can infer upper crustal composition during relatively short time intervals. Other methods used to determine upper crust composition typically give averages for 1 Ga time intervals. A major problem with the sediment approach is that elements such as Na, Ca, K, Ba, Sr, and Rb are mobile during sedimentary processes and therefore, their abundances in the sediments do not reflect their abundances in the source rocks.

Since the Libby Creek Group consists of passive margin sediments, it may provide a representative sampling of the composition of the Late Archean upper continental crust of the Wyoming Province. Pelites from the French Slate and diamictites from the Headquarters Formation are compared to a worldwide estimate of Late Archean upper crust obtained from map scaling. These samples were chosen because they show low quartz dilution effects. In terms of major elements, the Headquarters diamictites are very similar to the Late Archean Upper Crust (LAUC) compiled by Condie (1992) (Fig. 21). All of the major elements are within a factor of 1.5x of LAUC although some subtle differences occur. Ca and Na from the Headquarters Formation are lower than in LAUC and indicate that the source rocks of glacially derived sediments experienced some chemical weathering. In terms of major elements, pelites from the French Slate are more deviant from LAUC. Na and Ca are strongly depleted while K is enriched compared to LAUC. These anomalies are likely related to paleoweathering effects with Na and Ca being lost from the system due to the breakdown of plagioclase, while K is incorporated into clay minerals produced during the weathering of K-feldspars (Nesbitt et al., 1980). Other major element distributions in the French Slate are similar to LAUC and

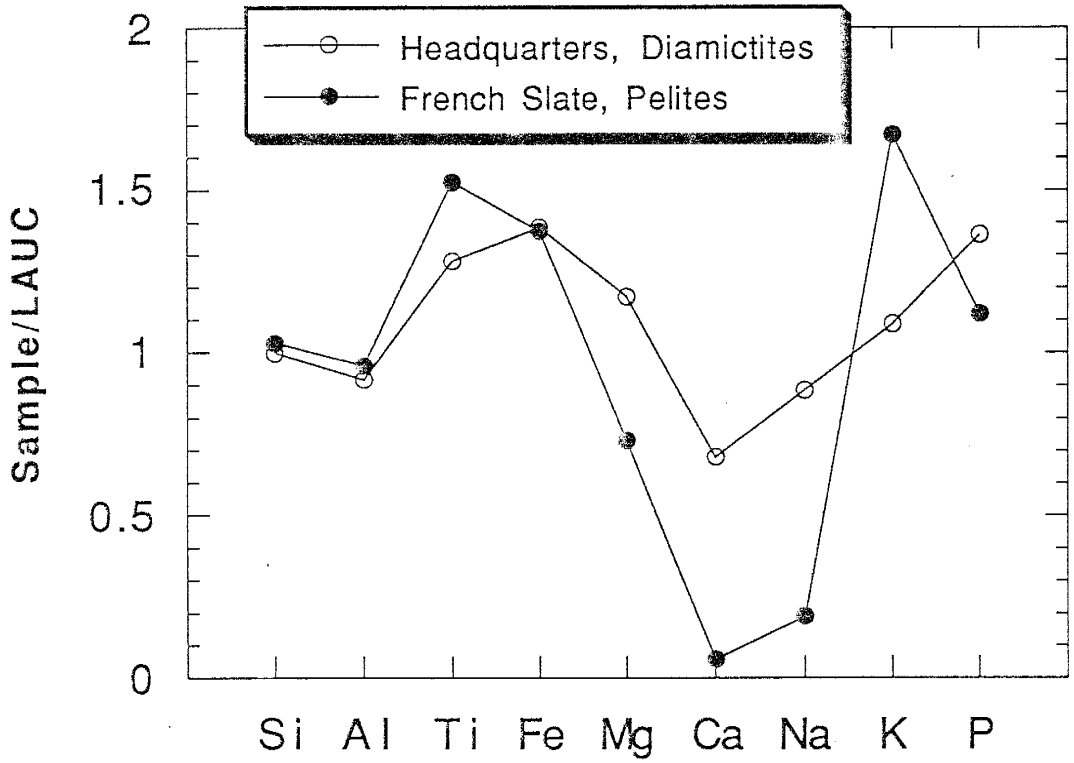

Figure 21. LAUC-normalized major element distributions for an average diamictite from the Headquarters Formation and an average pelite from the French Slate. LAUC (Late Archean Upper Crust) (Condie, 1992) composition given in Appendix C.

diamictites from the Headquarters Formation. It appears that for major elements, the diamictites provide a better estimate of crustal composition than do the pelites.

Trace element distributions in the Headquarters diamictites and French Slate pelites are also similar to LAUC (Fig. 22). Ba and Sr are depleted relative to LAUC for both the Headquarters Formation and the French Slate, a feature likely related to loss of feldspars. The diamictites from the Headquarters Formation are also depleted in Th and La possibly reflecting less granite in its source area than used in compiling LAUC. Cr and Ni in the French Slate are depleted, which may show less basalt and komatiite was present in its source area than in LAUC. The REE patterns of LAUC and the French Slate are similar in slope and abundances (Fig. 23). The French Slate has a slightly larger negative Eu anomaly and higher HREE. The Headquarters REE pattern shows a smaller negative Eu anomaly and lower LREE abundances than LAUC (Fig. 23), which could be explained by the presence of more granite in LAUC than in the source of the Headquarters sediments. Relative to LAUC, trace elements which are depleted in the Headquarters Formation are enriched in the French Slate, and vice versa (except for Ba and Sr). This may be a consequence of the length of the time that the LAUC average represents (1 Ga) compared to shorter time intervals represented by the sediments. During the Late Archean, K-rich granites became important constituents of the upper crust, significantly changing its composition (Taylor and McLennan, 1985). As demonstrated previously, the Headquarters Formation was deposited before K-rich granites became important in the Wyoming Province and the French Slate was deposited after they became important. The LAUC averages the composition of the upper crust over 1 Ga and does not

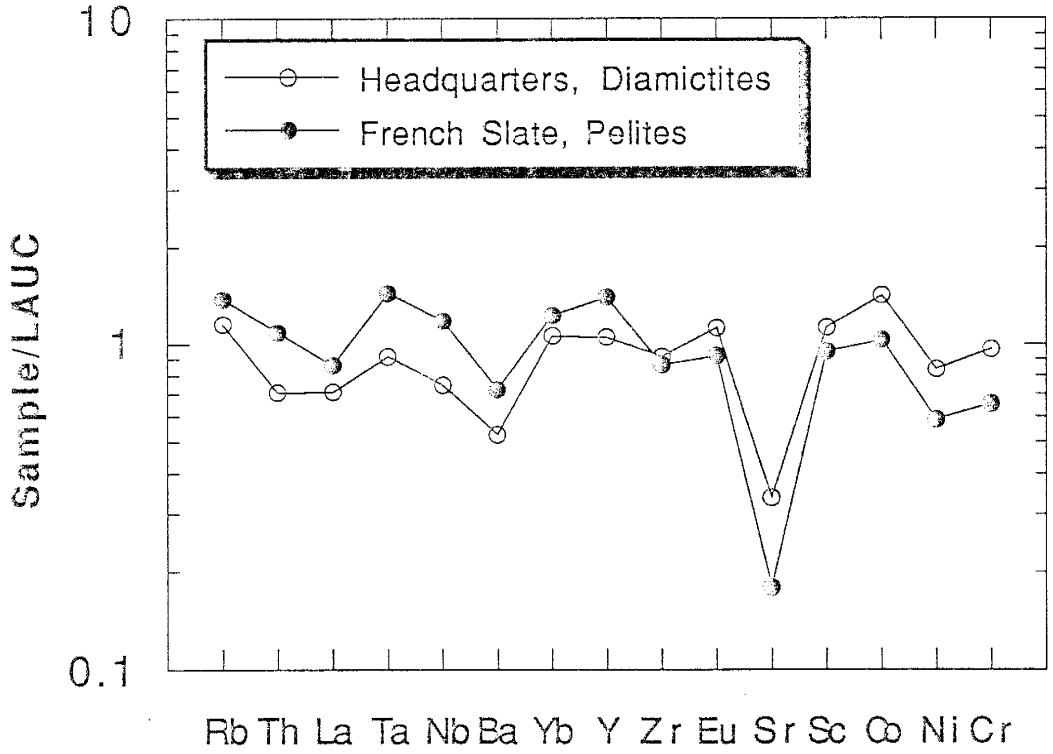

Figure 22. LAUC-normalized trace element distributions for an average diamictite from the Headquarters Formation and an average pelite from the French Slate. LAUC (Late Archean Upper Crust) (Condie, 1992) composition given in Appendix C.

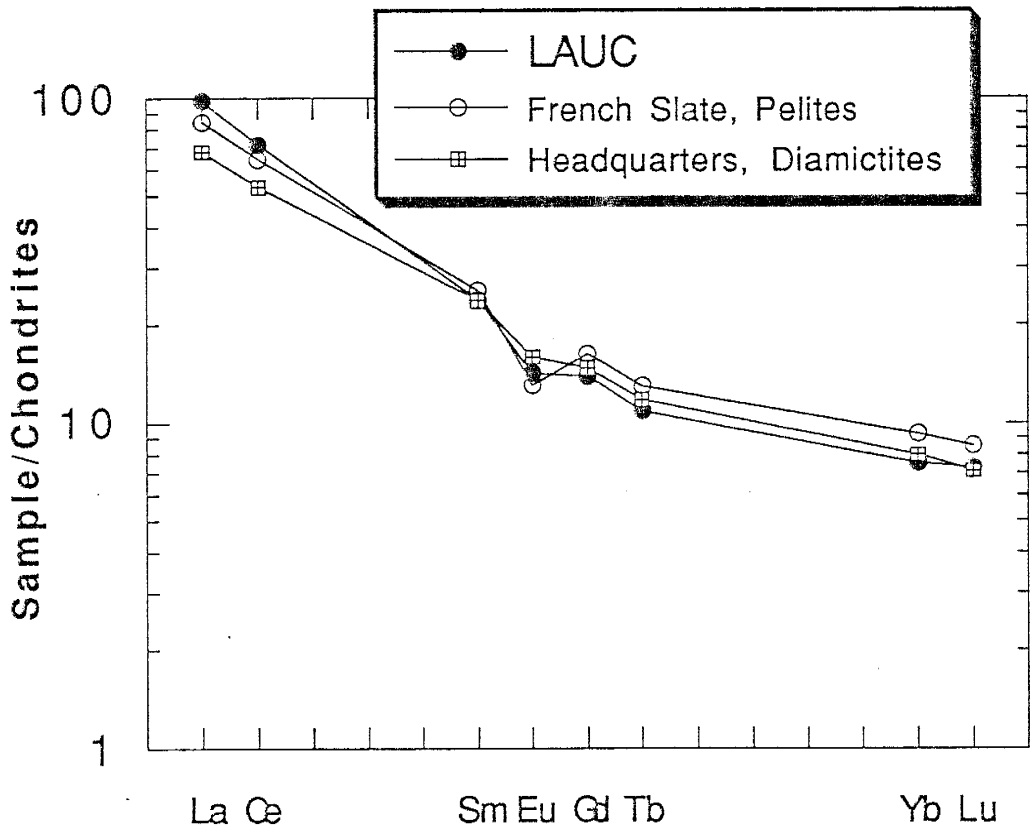

Figure 23. Chondrite-normalized REE distributions for an average diamictite from the Headquarters Formation, an average pelite from the French Slate and LAUC. LAUC (Late Archean Upper Crust) (Condie, 1992) composition given in Appendix C. Chondrite values are from Haskin et al. (1968) and are also given in Appendix C.

differentiate between upper crust composition before and after this event . Consequently, an average of the fine-grained sediments from the Headquarters Formation and French Slate provides a closer fit to the LAUC for trace elements and REE. This seems to indicate that both methods (map scaling and sediment composition) give reliable estimates of the composition of the upper crust. The composition of the Late Archean Upper Crust for the Wyoming Province, as determined by a mixture of the fine-grained sediments of the upper and lower Libby Creek Group, is given in Table 2. Concentrations of Ca, Na, K, Sr,. and Ba have not been determined from sediment chemistry due to their mobile nature, but are derived from the mixing calculations discussed previously.

These values represent only a first approximation of the composition of the Late Archean upper crust in the Wyoming Province and should be regarded as such.

CONCLUSIONS

The following conclusions have been reached in this study:

1) The use of quartzite geochemistry as a provenance indicator must be approached with caution, but can provide significant information about source rocks.

2) Mineral separate data indicate that the trace elements Th, U, Sc, Cr, Co and REE are mainly contained within micas (originally clays) of the Medicine Peak Quartzites. Zircon controls about 60% of the Hf in the whole rock, but only about 20% of the U and the HREE. Sphene is important only in controlling Ta.

3) The distributions of Fe, Ti, Sc, Co, Ni, and Cr in the Libby Creek quartzites appear to have been altered by some secondary process or

Table 2. Composition of the Late Archean Upper Crust of the Wyoming Province as determined from the fine-grained sediments of the Libby Creek Group. Major elements are in weight percent, trace elements are in ppm. Total Fe represented as Fe_2O_3-T.

SiO_2	67.55	Nb	8.46
Al_2O_3	14.01	Y	23.4
TiO_2	0.65	Zr	139
Fe_2O_3-T	5.66	Hf	3.42
MgO	2.28	Co	23
CaO	4.64	Ni	41
Na_2O	3.42	Cr	93
K_2O	2.62	Sc	12.9
P_2O_5	0.14	La	25.2
		Ce	51.8
Rb	125	Sm	4.42
Sr	253	Eu	1.0
Ba	567	Gd	3.85
Th	8.67	Tb	0.58
U	2.61	Yb	1.73
Ta	0.79	Lu	0.27

processes. It is possible that this process was diagenetic loss of Fe-Ti oxides through intrastratal solution.

4) A change in provenance occurred between the deposition of the Medicine Peak Quartzite and Lookout Schist, and has been identified using trace elements. The sources of the Headquarters, Heart, and Medicine Peak Formations appear to have been more mafic in overall composition than the sources of the Lookout Schist, Sugarloaf Quartzite and French Slate. This provenance change is not detectable using standard petrographic or field methods.

5) Paleoweathering indices suggest that the climate changed from cold (glacial) during the deposition of the Headquarters Formation to tropical during the deposition of the French Slate.

6) Mixing calculations indicate sediments from the Headquarters, Heart, and Medicine Peak Formations are derived from sources containing more TTG and basalt and less granite than sediments from the Lookout Schist, Sugarloaf Quartzite, and French Slate.

7) The Libby Creek Group shows similar secular geochemical trends to other Early Proterozoic basins, both of which are likely related to the widespread development of K-rich granites during the Late Archean.

Appendix A
Sampling, Sample Preparation, and Analytical Techniques

A total of 85 samples were collected with 38 being selected for chemical analysis (see Figure A-1 for sample locations). Each sample consisted of three specimens : one for reference, one for thin section, and one for chemical analysis. Samples were collected away from dikes and mineralized zones present in the Libby Creek Group in order to avoid their possible effects on primary sediment chemistry. Approximately 2 kilograms of sample were collected for chemical analysis to ensure a representative grain population. The sample chosen for chemical analysis was broken into small chips (1 to 2 cm) at the outcrop with weathered and altered portions being discarded. At New Mexico Tech the samples were powdered to a size of approximately 200 mesh in three steps. If needed, the samples were first passed through an electric chipmunk jar crusher. Next, samples were milled, using a rotary grinder with ceramic plates, to about the size of fine-grained sand. Samples that were less than the size of fine-grained sand were powdered in a high-speed agate mortar and pestle. Samples that remained coarser than fine-grained sand were powdered in a TEMA mill and were contaminated with W, Co and Ta. Correction factors for Co and Ta contamination were obtained by analyzing some samples in duplicate; one of the duplicates was ground in the TEMA mill and the other was ground in an agate mortar and pestle. It was found that the TEMA mill contains about 83% W, 17% Co, and 0.3% Ta. Corrections for Co and Ta contamination were made by multiplying the W value of the sample by 0.17 and 0.003 respectively and then subtracting this amount from the total Co and Ta (Table A-1). Co and Ta are not reported for samples that contain

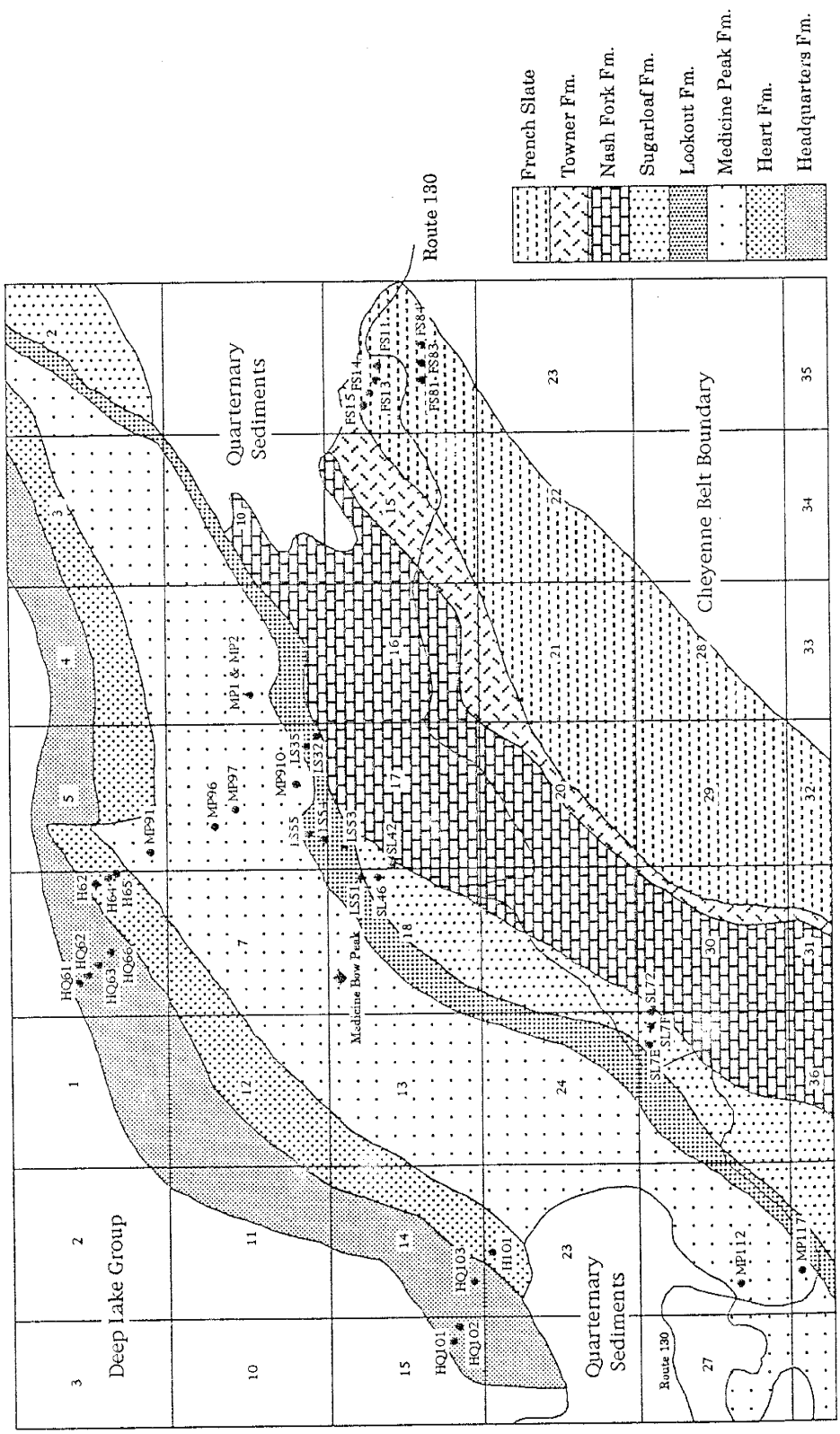

Figure A-1. Map showing the location of samples that were chemically analyzed. Each filled circle represents a sample location. (Modified from Houston et al., 1968).

greater than 250 ppm W contamination. The Co and Ta values for samples ground in the TEMA mill are suspect.

Table A-1. Co and Ta corrections.

Sample	W	Co-total	Co-corrected	Ta-total	Ta-corrected
LS35	122	24	3	0.87	0.5
LS51	166	32	4	1.4	0.9
LS55	95	24	8	0.9	0.6
MP910	200	36	2	0.86	0.3
H101	110	25	6	0.73	0.4
HQ102	189	40	8	1.2	0.6
HQ103	210	44	8	1.3	0.7

Thin sections were made of 14 samples which were stained with sodium cobaltinitrate to aid in the identification of K-feldspar. Modal analyses were performed using standard point counting techniques.

Approximately 10 kilograms of sample was collected for mineral separates. The sample was crushed in an electric chipmunk jar crusher and then was ground with a rotary grinder equipped with ceramic plates. The sample was then sieved to 40, 60, 80, 100, and 120 mesh sizes. Each size fraction was placed in an ultrasound for 15 minutes to break up multiple grains. The 100-120 mesh fraction (0.125-0.149 mm) contained the fewest grain aggregates and was used for heavy liquid separation. The quartz-mica fraction was separated from the heavy minerals using methylene iodide with a specific gravity of 3.3 g/cm^3. Quartz and mica were separated using a paper shaking technique. The heavy mineral fraction consisted

dominantly of zircon and sphene which were separated by hand-picking under a binocular microscope. The purity of the quartz, mica and sphene fraction are estimated to be greater than 95%, while the purity of the zircon fraction is about 77%.

Analytical Techniques

The abundances of the trace elements Hf, Ta, Sc, Co, Ni, Cr, Ba, Th, U, Cs, La, Ce, Nd, Sm, Eu, Tb, Yb, and Lu were determined by INAA (Instrumental Neutron Activation Analysis) using methods similar to those described by Jacobs et al. (1977) and Gibson and Jagan (1977). Approximately 300 mg of the powdered sample were heat sealed in polyethylene vials which were then irradiated at the Annular Core Research Reactor at Sandia National Laboratory in Alburquerque, New Mexico. The samples were irradiated for ten thousand seconds. An air hose attached to the sample canister in the reactor blew the vials around to ensure an equivalent neutron flux for each sample. At New Mexico Tech, 7 and 40 days after irradiation, gamma-ray emissions were counted for each sample using two-coaxial Ge detectors. Data reduction is performed using TEABAGS (Trace Element Analysis By Automated Gamma-ray Spectrometry) (Lindstrom and Korotev 1982) software run on a VAX computer. A fly ash standard NIST-SRM-1633a was analyzed in triplicate and was used as a calibrating standard. Additional rock standards, AN-G (anorthosite), G-2 (granite) and AGV-1 (andesite) were analyzed as unknowns (check standards) to help determine the precision and accuracy of the run. The samples FS11 (pelite), SL7E (quartzite), and MP96 (quartzite) were also analyzed multiply to aid in the determination of precision for both INAA and XRF.

Major and trace elements Rb, Sr, Y, Zr, and Nb were determined by XRF (X-ray Fluorescence) using an automated 3064 XRF spectrometer with data reduction being performed with a PDP-11 computer using in-house software at the New Mexico Bureau of Mines and Mineral Resources. Major elements are determined on fusion discs following the methods of Norrish and Hutton (1969). Fusion discs are made by fusing about 0.5 grams of sample powder with about 2.7 grams of Spectroflux-105 (a glass formed from lithium tetraborate, lithium carbonate, and lanthanum oxide) along with several beads of NH_4NO_3 (oxidant). The mixture was then heated in a Pt crucible over an open flame until molten. This was poured into a mold, and the fusion discs were gradually cooled and subsequently analyzed.

Trace elements are analyzed using pressed powder pelites following the procedures of Norrish and Chappel (1977). About 7 grams of sample powder along with 7 drops of polyvinyl alchohol (a binder) is backed with boric acid and pressed with 20 tons of pressure for about one minute.

Tables A-2 through A-5 give precisions and accuracies for INAA and XRF obtained in this study.

Table A-2. Precision and accuracy for INAA determined from AN-G.

	AN-G a	AN-G b	AN-G c	x*	s^	C.V.#	AN-G accepted~	Percent accuracy$
Sc	10.2	10.2	10.2	10.2	0	0	10	2.0
Cr	49	48	49	49	0.58	1.2	50	2.0
Co	28.7	27.7	25.9	27.4	1.16	4.23	25	9.6
Ni	33	41	39	38	4.16	10.9	35	8.6
Cs	0.10	0.08	0.06	0.08	0.02	25	0.06	33
Ba	37	39	34	37	2.5	6.8	34	8.8
Hf	0.40	0.36	0.47	0.41	0.045	10.98	0.38	7.3
Ta	0.16	0.21	0.20	0.19	0.020	10.42	0.2	5.0
Th	0.03	0.07	0.03	0.04	0.023	57.5	0.04	0
U	n.d.	0.1	0.1	0.1	0	0	-------	-------
La	2.35	2.35	2.27	2.32	0.038	1.64	2	16.0
Ce	5.25	4.77	4.99	5.00	0.196	3.92	4.7	6.38
Nd	3	2	3	3	0.58	19.3	2.4	0.25
Sm	0.76	0.82	0.81	0.80	0.032	4.0	0.7	14.3
Eu	0.37	0.37	0.37	0.37	0	0	0.37	0
Tb	0.19	0.22	0.20	0.20	0.015	7.5	0.2	0
Yb	0.84	0.85	0.97	0.89	0.072	8.1	0.85	4.7
Lu	0.12	0.12	0.12	0.12	0	0	0.12	0

* - Mean value of AN-G this study.
^ - One standard deviation of x.
# - Coefficient of variation = (s/x) X 100.
~ - Accepted values of AN-G from Govindaraju (1989).
$ - % Accuracy = [(|x - actual|) /actual] X 100.
Samples irradiated 11/9/90.

Table A-3. Accuracy for INAA determined from AG-V and G-2.

	AG-V This Study	AG-V Accepted*	% accuracy#	G-2 This Study	G-2 Accepted*	% accuracy#
Sc	11.8	12.2	3.28	3.4	3.5	2.9
Cr	10	10.1	1.0	7	8.7	19.5
Co	15.7	15.3	2.61	4.5	4.6	2.2
Ni	18	16	11.1	3	5	40
Cs	1.38	1.28	7.81	1.53	1.34	14.2
Ba	1385	1226	13.0	2206	1882	17.2
Hf	5.6	5.1	9.8	9.0	7.9	13.9
Ta	0.97	0.90	7.8	0.89	0.88	1.14
Th	6.5	6.5	0	26.3	24.7	6.48
U	2.3	1.92	19.8	2.4	2.07	15.9
La	39.2	38	3.16	91	89	2.2
Ce	68.5	67	2.24	167	160	4.38
Nd	36	33	9.1	59	55	7.27
Sm	6.3	5.9	6.8	8.1	7.2	12.5
Eu	1.7	1.64	3.7	1.5	1.4	7.1
Tb	0.74	0.7	5.7	0.51	0.48	6.3
Yb	1.8	1.72	4.7	0.77	0.8	3.8
Lu	0.25	0.27	7.4	0.11	0.11	0

* - Accepted values from Govindaraju (1989).
# - % Accuracy = [(|x - accepted|)/accepted] X 100.
Samples irradiated 11/9/90.

Table A-4. Precision for INAA and XRF determined from sample FS11 (pelite).

INAA	FS11a	FS11b	FS11c	x*	s #	C.V.~
Fe_2O_3-T	4.39	4.52	4.60	4.50	0.11	2.44
Sc	15.2	15.5	15.9	15.5	0.278	1.79
Cr	126	128	132	129	3.06	2.4
Co	12.5	13.1	13.2	12.9	0.288	2.23
Ni	20	39	40	33	11.3	3.42
Rb	137	138	145	140	4.35	3.11
Cs	6.4	6.5	6.7	6.5	0.131	2.01
Ba	338	349	352	346	6.02	1.74
Hf	3.45	3.56	3.49	3.50	0.045	1.29
Ta	1.06	1.05	1.09	1.07	0.017	1.59
Th	12.4	12.7	13.1	12.8	0.302	2.37
U	2.0	2.3	2.2	2.2	0.15	6.8
La	35.5	36.3	37.2	36.3	0.694	1.91
Ce	67.4	68.2	69.8	68.5	0.998	1.46
Nd	27	28	32	29	2.6	9.0
Sm	5.7	5.8	6.0	5.8	0.153	2.6
Eu	1.17	1.19	1.21	1.19	0.016	1.34
Tb	0.71	0.74	0.74	0.73	0.018	2.47
Yb	2.02	2.04	2.04	2.03	0.012	0.59
Lu	0.26	0.28	0.30	0.28	0.020	7.17
XRF						
SiO_2	65.52	64.84	65.22	65.19	0.278	0.43
TiO_2	1.00	0.99	0.97	0.98	0.013	1.32
Al_2O_3	18.81	18.67	18.64	18.71	0.074	0.40
Fe_2O_3-T	5.72	5.63	5.65	5.67	0.040	0.71
MnO	0.046	0.036	0.042	0.041	0.004	9.76
MgO	2.02	1.79	1.82	1.88	0.101	5.37
CaO	0.23	0.24	0.23	0.24	0.003	1.28
Na_2O	0.61	0.51	0.57	0.56	0.044	7.82
K_2O	4.65	4.63	4.66	4.65	0.012	0.26
P_2O_5	0.10	0.10	0.10	0.10	0	0
Rb	157	158	156	157	1	0.64
Sr	66	65	65	65	0.58	0.89
Y	30	29	29	29	0.58	2.0
Zr	151	151	149	150	1.2	0.8
Nb	11	10	11	11	0.58	5.3

* - Mean value of FS11.
# - One standard deviation of the mean.
~ - Coefficient of variation = (x/s) X 100.
Samples irradiated 11/9/90.

Table A-5. Precision for INAA and XRF determined from sample SL7E (quartzite).

INAA	SL7Ea	SL7Eb	x	s	C.V.
Fe_2O_3-T	0.06	0.06	0.06	0	0
Sc	0.2	0.2	0.2	0	0
Cr	2	2	2	0	0
Ni	0.4	1.4	0.90	0.500	55.6
Cs	0.06	0.05	0.06	0.007	11.7
Ba	8	5	6	2.1	35
Hf	0.81	1.02	0.92	0.15	16.3
Th	1.83	1.84	1.84	0.007	0.38
U	0.4	0.4	0.4	0	0
La	9.75	10.07	9.91	0.160	1.61
Ce	18.0	18.8	18.4	0.375	2.04
Nd	6	8	7	1.41	20.1
Sm	1.19	1.20	1.20	0.007	0.58
Eu	0.16	0.16	0.16	0	0
Tb	0.07	0.10	0.08	0.02	25
Yb	0.25	0.30	0.28	0.035	12.5
Lu	0.04	0.04	0.04	0	0
XRF					
Rb	5.9	6.6	6.3	0.49	7.8
Sr	6.2	6.0	6.1	0.135	2.21
Y	2.0	1.9	2.0	0.071	3.6
Zr	37	42	40	3.5	8.8
Nb	n.d.	n.d.	n.d.	------	-----

See footnote for Table A-3.

Table A-6. Precision for INAA and XRF determined from sample MP91 (quartzite).

INAA	MP91a	MP91b	x	s	C.V.
Fe_2O_3-T	0.10	0.09	0.10	0.007	7.0
Sc	0.36	0.34	0.35	0.014	4.0
Cr	12	12	12	0	0
Ni	3	1.0	2	1.4	70
Cs	0.08	0.06	0.07	0.014	20
Ba	22	20	21	1.00	4.76
Hf	0.95	0.86	0.91	0.064	7.03
Th	1.74	1.65	1.70	0.064	3.76
U	0.2	0.2	0.2	0	0
La	4.78	4.41	4.60	0.185	4.02
Ce	9.11	7.91	8.51	0.60	7.05
Nd	2	4	3	1.4	46.7
Sm	0.42	0.40	0.41	0.014	3.41
Eu	0.08	0.08	0.08	0	0
Tb	0.04	0.03	0.04	0.007	17.5
Yb	0.16	0.16	0.16	0	0
Lu	0.02	0.02	0.02	0	0
XRF					
Rb	26	27	26	0.71	2.73
Sr	13	13	13	0	0
Y	n.d.	n.d.	-----	-----	-----
Zr	35	33	34	0.71	2.09
Nb	n.d.	n.d.	-----	-----	-----

See Table A-3 footnote.

Appendix B
Chemical Analyses of Libby Creek Sediments

Table B-1. Chemical analyses of pelites and diamictites from the Libby Creek Group.

	Pelites						
	FS11	FS13	FS14	FS81	FS83	FS84	ND21
SiO_2	65.19	68.95	66.22	77.28	75.71	57.64	62.68
TiO_2	0.98	0.78	0.86	0.59	0.49	0.49	0.50
Al_2O_3	18.71	15.45	15.92	12.91	12.43	10.42	17.42
Fe_2O_3-T	5.67	6.27	7.70	2.15	3.69	16.33	6.19
MnO	0.041	0.029	0.040	0.019	0.025	0.025	0.025
MgO	1.88	2.34	2.69	1.09	1.23	1.11	3.89
CaO	0.24	0.23	0.25	0.21	0.17	0.18	0.25
Na_2O	0.56	0.64	0.49	0.78	0.88	0.88	2.36
K_2O	4.65	4.22	4.42	4.54	3.93	3.40	6.56
P_2O_5	0.10	0.10	0.13	0.12	0.12	0.17	0.11
LOI	1.73	1.51	3.73	1.20	3.18	9.97	2.73
TOTAL	99.75	100.52	102.45	100.89	101.86	100.61	102.72
Rb	157	145	140	138	126	110	151
Ba	346	323	250	973	394	349	691
Cs	6.5	5.1	4.4	4.6	4.2	3.6	3.3
Sr	65	32	16	72	88	81	15
Th	12.8	10.3	10.6	8.71	10.9	10.1	10.7
U	2.2	2.0	5.4	2.3	3.8	2.1	1.6
Sc	15.5	13.0	14.7	9.77	9.43	8.70	10.2
Cr	129	84	93	46	55	47	76
Co	12.9	16.8	17.2	12.6	26.5	33.2	17.8
Ni	33	23	29	18	35	81	41
Y	29	22	26	24	29	32	7.1
Zr	150	153	159	112	128	111	116
Nb	11	8	11	7	11	13	9
Hf	3.5	3.5	3.4	2.4	2.8	2.3	2.5
Ta	1.1	0.93	0.96	0.79	1.0	1.0	0.88
La	36.3	26.3	25	25.4	31.8	22.2	24.1
Ce	68.5	50.2	44.7	56.1	76.1	47.3	46.2
Sm	5.8	4.3	3.9	4.4	5.4	4.0	3.1
Eu	1.19	0.88	0.85	0.82	0.93	0.76	0.59
Tb	0.73	0.55	0.52	0.57	0.67	0.65	0.23
Yb	2.03	1.5	1.5	1.8	2.2	2.4	0.44
Lu	0.28	0.22	0.24	0.29	0.34	0.40	0.07
Eu/Eu*	0.69	0.68	0.71	0.62	0.57	0.58	0.76
$(La/Yb)_n$	13.1	10.7	9.9	8.4	8.8	5.6	33.6
CIW	93.0	91.3	92.7	88.6	87.6	85.4	80.1

* See footnote at the end of Table B-1.

Table B-1 continued.

	Pelites						
	LS51^	LS54	LS55^	LS35^	MP910^	H101^	HQ62
SiO_2	81.16	83.14	79.06	73.82	85.12	74.22	85.71
TiO_2	0.28	0.31	0.32	0.31	0.14	0.24	0.36
Al_2O_3	10.78	9.90	10.43	13.75	9.85	11.88	8.13
Fe_2O_3-T	1.59	1.52	2.25	3.50	0.66	1.53	1.15
MnO	0.017	0.017	0.022	0.037	0.012	0.027	0.015
MgO	0.70	0.49	0.84	1.30	0.33	0.78	0.58
CaO	0.17	0.21	0.20	0.25	0.16	2.99	0.14
Na_2O	0.98	2.96	1.20	5.72	3.55	3.80	1.15
K_2O	3.14	1.51	2.97	1.30	1.27	2.08	2.30
P_2O_5	0.08	0.05	0.06	0.08	0.03	0.08	0.07
LOI	1.75	0.80	2.07	1.19	0.97	3.30	0.99
TOTAL	100.64	100.91	99.42	101.25	102.09	100.93	100.59
Rb	107	58	123	55	39	71	70
Ba	171	85	601	105	516	279	347
Cs	2.8	2.3	4.6	1.7	0.42	1.1	0.63
Sr	18	30	25	40	27	61	25
Th	12.7	9.15	8.51	7.55	4.25	2.94	5.22
U	2.8	2.9	1.8	2.1	1.3	1.3	1.7
Sc	2.9	5.5	6.6	2.1	1.1	3.7	4.8
Cr	50	43	26	37	12	33	67
Co	4	4.9	8	3	2	6	6.1
Ni	13	14	n.d.	16	10	13	7
Y	36	34	18	28	12	7	7
Zr	256	144	114	337	237	95	94
Nb	8	6	7	7	n.d.	n.d.	n.d.
Hf	5.9	3.9	2.7	7.4	5.5	2.2	2.2
Ta	0.9	0.45	0.6	0.5	0.3	0.4	0.27
La	83	21.6	19.9	33.8	21.8	8.99	8.0
Ce	191	45.5	35.7	83.4	42	18.4	15.2
Sm	18.6	3.7	2.5	8.1	3.9	1.7	1.5
Eu	2.2	0.82	0.37	1.5	0.72	0.41	0.37
Tb	2.4	0.67	0.34	0.73	0.44	0.19	0.17
Yb	4.4	2.7	1.4	2.0	1.1	0.50	0.49
Lu	0.57	0.46	0.23	0.30	0.17	0.08	0.08
Eu/Eu*	0.40	0.66	0.48	0.67	0.63	0.86	0.84
$(La/Yb)_n$	11.5	4.8	8.6	10.3	11.9	10.9	9.8
CIW	84.9	65.3	81.7	58.2	61.6	50.4	79.1

* See footnote at end of Table B-1.

Table B-1 continued.

	Pelites		Diamictites	
	HQ102^	HQ103^	HQ66	HQ101
SiO_2	80.82	65.20	64.72	68.37
TiO_2	0.18	0.67	0.61	0.56
Al_2O_3	10.83	16.14	12.20	15.20
Fe_2O_3-T	1.03	8.00	9.16	4.91
MnO	0.050	0.13	0.22	0.058
MgO	0.44	2.70	3.35	2.24
CaO	1.37	0.74	4.0	0.93
Na_2O	3.59	4.06	1.85	4.81
K_2O	1.96	2.46	3.33	2.12
P_2O_5	0.45	0.13	0.13	0.17
LOI	0.50	0.60	1.05	1.04
TOTAL	100.82	100.83	100.62	100.41
Rb	69	103	148	78
Ba	161	179	320	318
Cs	0.55	0.55	7.0	1.8
Sr	51	88	143	79
Th	2.6	2.8	6.1	7.6
U	1.32	0.78	2.27	2.28
Sc	2.8	3.0	16	12
Cr	39	42	106	116
Co	8	8	31	22.7
Ni	7	4	5	4
Y	6	17	26	14
Zr	166	145	138	148
Nb	n.d.	9	7	6
Hf	4.4	4.8	3.7	4.1
Ta	0.6	0.7	0.46	0.76
La	7.29	7.58	19.2	25.8
Ce	14.0	15.8	40.4	52.8
Sm	1.2	1.4	4.3	4.1
Eu	0.31	0.39	1.2	1.0
Tb	0.13	0.18	0.70	0.41
Yb	0.54	0.57	1.9	1.3
Lu	0.09	0.09	0.28	0.19
Eu/Eu*	0.88	0.93	0.85	0.88
$(La/Yb)_n$	8.2	8.1	6.1	12.2
CIW	56.3	66.8	54.2	61.3

^ Samples ground in a TEMA mill.

Fe_2O_3-T, Total Fe as Fe_2O_3; major elements in weight percent; trace elements in ppm; n.d., not detected; $Eu/Eu^* = Eu_n/(Sm_n \times Gd_n)^{1/2}$; $Gd_n = (Sm_n \times Tb_n^2)^{1/3}$; CIW = $[Al_2O_3/(Al_2O_3 + CaO + NaO)] \times 100$ in molecular proportions. FS = French Slate, SL = Sugarloaf Quartzite, LS = Lookout Schist, MP = Medicine Peak Quartzite, H = Heart, HQ = Headquarters Schist.

Table B-2. Chemical analyses of quartzites from the Libby Creek Group.

	Quartzites						
	FS15^	SL42^	SL46	SL72	SL7F^	SL7E	LS32^
SiO_2	96.47	98.73	98.84	98.05	98.55	98.62	98.77
TiO_2	0.02	0.02	0.03	0.03	0.04	0.04	0.03
Al_2O_3	1.11	1.13	1.09	0.84	1.10	1.09	1.17
Fe_2O_3-T	0.57	0.08	0.08	0.07	0.10	0.08	0.14
MnO	0.025	0.014	0.014	0.010	0.013	0.012	0.011
MgO	0.40	0.075	0.03	0.02	0.22	n.d.	0.03
CaO	1.43	0.11	0.11	0.12	0.12	0.12	0.11
Na_2O	0.32	0.19	0.17	0.14	0.35	0.19	0.21
K_2O	0.01	0.12	0.05	0.06	0.10	0.12	0.18
P_2O_5	0.05	0.03	0.03	0.03	0.03	0.03	0.02
LOI	1.53	0.099	0.114	0.050	0.23	0.080	0.12
TOTAL	101.94	100.60	100.55	99.42	100.85	100.39	100.80
Rb	3.2	7.0	5.0	5.1	5.5	6.3	5.0
Ba	13	n.d.	17	16	8	6	20
Cs	0.06	0.04	0.05	0.06	0.05	0.06	0.09
Sr	13	5.5	5.3	5.5	6.0	6.1	3.3
Th	0.58	1.1	1.5	1.8	2.1	1.84	0.84
U	0.5	0.3	0.3	0.3	0.3	0.4	0.3
Sc	0.26	0.21	0.10	0.11	0.17	0.20	0.18
Cr	4	2	2	2	2	2	1
Co			0.06	0.06		0.07	
Ni	n.d.	2	n.d.	n.d.	n.d.	n.d.	n.d.
Y	2.9	3.0	3.6	2.6	2.3	2.0	2.6
Zr	14	35	21	29	28	40	34
Nb	n.d.	n.d.	n.d.	n.d.	n.d.	n.d.	n.d.
Hf	0.26	0.77	0.53	0.57	0.72	0.92	0.82
Ta			0.08	0.08		0.09	
La	0.78	5.84	9.0	6.94	8.85	9.91	3.05
Ce	1.40	11.3	17.8	14.9	17.0	18.4	6.04
Sm	0.14	0.81	1.4	0.98	1.3	1.2	0.40
Eu	0.30	0.17	0.22	0.13	0.18	0.16	0.06
Tb	0.07	0.12	0.13	0.01	0.11	0.08	0.05
Yb	0.10	0.22	0.30	0.14	0.18	0.28	n.d.
Lu	0.02	0.03	0.04	0.02	0.03	0.04	0.02
Eu/Eu*	4.6	0.68	0.60	0.46	0.53	0.52	0.52
$(La/Yb)_n$	4.7	16.1	18.3	30.2	30.1	25.6	-----
CIW	26.2	68.8	69.4	65.2	58.1	67.3	68.2

* See footnote at end of Table B-1.

Table B-2 continued.

	Quartzites						
	LS53^	MP97^	MP96	MP117^	MP112	MP1	MP2
SiO_2	92.38	-----	97.36	97.66	95.25	91.80	90.67
TiO_2	0.35	-----	0.03	0.03	0.02	0.22	0.14
Al_2O_3	5.06	-----	1.60	1.71	3.31	5.84	6.45
Fe_2O_3-T	0.33	-----	0.13	0.061	0.13	0.25	0.19
MnO	0.013	-----	0.011	0.009	0.005	0.008	0.008
MgO	0.23	-----	n.d.	0.01	0.17	0.08	0.09
CaO	1.0	-----	0.11	0.11	0.12	0.12	0.11
Na_2O	2.57	-----	0.40	0.35	0.27	0.30	0.42
K_2O	0.03	-----	0.22	0.30	0.79	1.52	1.52
P_2O_5	0.04	-----	0.02	0.03	0.02	0.04	0.03
LOI	0.20	-----	0.31	0.20	0.40	0.74	0.85
TOTAL	102.20	-----	100.19	100.46	100.49	100.92	100.48
Rb	4.1	4.6	8.3	9.1	25	42	39
Ba	n.d.	15	29	20	14	18	22
Cs	0.06	0.10	0.08	0.05	0.14	0.20	0.19
Sr	8.9	7.1	6.0	6.0	7.3	30	27
Th	6.3	1.4	2.1	2.1	1.9	5.4	4.2
U	1.4	0.2	0.2	0.4	0.4	0.7	0.7
Sc	1.18	0.26	0.68	0.24	0.48	2.30	2.59
Cr	57	4	13	5	12	235	176
Co			0.24		0.14	0.26	0.21
Ni	n.d.	6	3	n.d.	4	10	7
Y	23	1.1	2.4	0.7	1.2	2.1	3.9
Zr	526	33	37	32	29	193	129
Nb	5	n.d.	n.d.	n.d.	n.d.	n.d.	n.d.
Hf	12	0.78	1.2	0.63	0.65	6.0	3.2
Ta			0.09		0.08	0.43	0.41
La	20.5	4.64	7.99	11.1	4.48	10.5	10.7
Ce	46.3	7.6	11.8	22.3	8.18	21.5	19.7
Sm	5.7	0.50	0.57	1.1	0.63	1.4	1.4
Eu	1.0	0.12	0.14	0.21	0.12	0.30	0.32
Tb	0.73	0.08	0.09	0.06	0.06	0.11	0.15
Yb	1.8	0.14	0.35	0.14	0.16	0.47	0.57
Lu	0.25	n.d.	0.06	0.03	0.02	0.08	0.10
Eu/Eu*	0.59	0.72	0.75	0.87	0.73	0.82	0.80
$(La/Yb)_n$	7.0	19.5	13.7	48.9	16.6	13.4	11.3
CIW	45.6	-----	65.1	68.8	83.3	89.1	87.9

* See footnote at end of Table B-1.

Table B-2 continued.

	Quartzites					
	MP91	H62^	H64	H65	HQ61	HQ63^
SiO_2	95.21	94.76	94.82	94.53	93.15	93.88
TiO_2	0.04	0.03	0.04	0.06	0.05	0.04
Al_2O_3	4.33	3.59	3.65	3.43	3.77	2.58
Fe_2O_3-T	0.13	0.31	0.49	0.71	0.23	1.02
MnO	0.013	0.008	0.01	0.012	0.015	0.03
MgO	n.d.	0.24	0.20	0.28	0.36	0.94
CaO	0.10	0.11	0.12	0.11	0.12	1.48
Na_2O	0.43	0.37	0.36	0.46	0.50	0.69
K_2O	0.98	0.83	0.47	0.77	1.96	0.02
P_2O_5	0.02	0.02	0.02	0.02	0.02	0.03
LOI	0.51	0.43	0.60	0.41	0.30	0.24
TOTAL	101.77	100.70	100.78	100.80	100.48	100.95
Rb	26	26	17	22	48	3.6
Ba	21	14	n.d.	11	185	13
Cs	0.07	0.15	0.11	0.17	0.22	0.01
Sr	13	9.2	12	11	15	40
Th	1.7	2.3	2.0	2.2	2.5	2.5
U	0.2	0.3	0.3	0.3	0.8	1.1
Sc	0.35	0.70	0.34	1.1	0.52	1.1
Cr	12	12	13	19	6	8
Co	0.1		0.77	2.1	1.2	
Ni	2	3	3	n.d.	n.d.	4
Y	n.d.	1.8	n.d.	n.d.	3.3	6.8
Zr	34	31	29	34	43	37
Nb	n.d.	n.d.	n.d.	n.d.	n.d.	n.d.
Hf	0.91	0.75	0.94	1.0	0.94	0.94
Ta	0.12		0.07	0.12	0.09	
La	4.60	5.01	7.11	3.63	8.35	3.21
Ce	8.51	8.6	9.36	7.2	16.0	6.09
Sm	0.41	0.57	0.43	0.39	1.1	0.88
Eu	0.08	0.12	0.10	0.11	0.22	0.30
Tb	0.04	0.05	0.04	0.06	0.09	0.23
Yb	0.16	0.16	0.17	0.19	0.30	0.54
Lu	0.02	0.03	0.03	0.03	0.05	0.08
Eu/Eu*	0.84	0.81	0.84	0.85	0.80	0.90
$(La/Yb)_n$	19.4	19.1	25.6	11.8	16.7	3.6
CIW	83.0	81.6	81.8	78.2	78.4	40.3

* See footnote at end of Table B-1.

Table B-3. Mineral Separates results for sample MP1. Trace elements reported in ppm.

	Sphene	Zircon	Fuchsite
Th	14	286	22.7
U	9	346	3.0
Hf	19	9420	7.3
Ta	70	6.0	1.5
La	11	80	34.7
Ce	14	502	72
Sm	2.0	154	4.7
Eu	1.1	62	1.1
Tb	0.90	44	0.41
Yb	4.0	252	2.0
Lu	0.60	47.6	0.30
Sc	9.8	133	14
Cr	8.7	326	1400
Co	9.4	52	1.2

Concentrations in the whole-rock are given in Table B-2.

Appendix C
Normalizing and Average Rock Compositions Used

Table C-1. Normalizing and mixing values used.

			Late Archean Averages			
	PAAS@	Chondrites#	U.C.*	TTG+	Granite+	Basalt+
SiO_2	62.8		66.62	69.50	72.40	50.50
TiO_2	1.0		0.46	0.34	0.25	0.97
Al_2O_3	18.9		14.93	15.10	14.80	15.00
Fe_2O_3-T	6.5		5.08	3.89	2.16	12.00
MgO	2.2		2.39	1.10	0.37	7.60
CaO	1.3		3.64	2.80	1.18	10.2
Na_2O	1.2		3.76	4.50	3.16	2.60
K_2O	3.7		2.51	2.40	4.94	0.33
P_2O_5	0.16		0.11	0.11	0.08	0.12
Rb	160		98	76	150	9.0
Sr	200		330	470	145	150
Ba	650		605	715	765	204
Th	14.6		9.65	7.20	15	0.60
U	3.1		2.41	1.60	3.50	1.00
Zr	210		157	156	155	98
Hf	5		3.94	4.00	4.50	1.80
Nb	19		8.76	9.00	12	5.00
Ta~	1.12		0.67	0.70	1.0	0.30
Y	27		19.1	12.0	20.0	23
La	38	0.33	32.3	30.0	50.0	5.5
Ce	80	0.88	63.1	56.0	95.0	15
Nd	32	0.60	26.5	22.0	46.0	9.6
Sm	5.6	0.181	4.31	3.60	6.30	2.8
Eu	1.1	0.069	0.98	1.00	0.85	1.0
Gd	4.7	0.249	3.47	2.26	4.67	3.57
Tb	0.77	0.047	0.51	0.29	0.65	0.65
Yb	2.8	0.200	1.51	0.64	2.0	2.5
Lu	0.43	0.034	0.25	0.11	0.32	0.42
Sc	16		12.4	4.0	4.0	35
Cr	110		115	22	16	406
Co	23		19	10	3.5	55
Ni	55		58.4	11.0	12.0	182

@ - PAAS values from Taylor and McLennan (1985).
~ - Ta is not reported for PAAS, value is from NASC Gromet et al. (1984).
# - Chondrite values from Haskin et al. (1968).
* - Late Archean Upper Crust average from Condie (1992).
+ - Unpublished compilation from the literature by K. C. Condie.

Table C-2. Formation averages and standard deviations.

	Quartzites									
	SL n=5		LS n=2		MP n=7		H n=3		HQ n=2	
	x	s	x	s	x	s	x	s	x	s
SiO_2	98.56	0.30	94.58	5.9	94.49	2.9	94.7	0.15	93.52	0.52
TiO_2	0.03	0.008	0.19	0.22	0.08	0.08	0.04	0.019	0.05	0.007
Al_2O_3	1.05	0.12	3.12	2.8	3.87	2.0	3.56	0.11	3.18	0.84
Fe_2O_3	0.08	0.01	0.24	0.13	0.15	0.06	0.50	0.20	0.63	0.56
MgO	0.07	0.09	0.13	0.14	0.06	0.07	0.24	0.04	0.65	0.41
CaO	0.12	0.006	0.56	0.63	0.11	0.008	0.11	0.006	0.80	0.96
Na_2O	0.21	0.08	1.39	1.67	0.36	0.07	0.40	0.06	0.60	0.13
K_2O	0.09	0.03	0.11	0.10	0.89	0.57	0.69	0.19	0.99	1.37
P_2O_5	0.03	0.003	0.03	0.009	0.03	0.008	0.023	0.002	0.03	0.003
Rb	5.9	0.91	4.6	0.59	22	15.2	21	4.5	26	31.1
Th	1.6	0.40	3.6	3.9	2.7	1.47	2.2	0.19	2.5	0.04
La	8.2	1.73	11.8	12.3	7.73	3.09	5.25	1.8	5.78	3.63
Ta	0.08	0.009	0.26	0.24	0.19	0.16	0.09	0.028	0.11	0.03
Nb			4.87	0						
Ba	14	4.9	20	0	20	5.07	13	1.45	99	121
Yb	0.22	0.06	1.77	0	0.28	0.18	0.17	0.014	0.42	0.16
Y	2.7	0.65	13	14.3	1.7	1.18	1.2	0.63	5.1	2.5
Zr	31	7.9	280	347	69	65.1	31	2.4	40	4.69
Eu	0.17	0.04	0.53	0.66	0.18	0.09	0.11	0.01	0.26	0.06
Sr	5.7	0.32	6.1	4.0	14	10.2	11	1.45	27	17.9
Sc	0.15	0.05	0.68	0.71	0.99	1.01	0.70	0.36	0.82	0.42
Co	0.06	0.008	2.5	3.4	0.20	0.062	1.30	0.70	1.5	0.43
Ni	2.2	0			5.5	2.75	2.9	0.35	3.9	0
Cr	1.7	0.19	29	39.2	65	97.4	15	3.87	6.9	1.27

SL = Sugarloaf Quartzite, LS = Lookout Schist, MP = Medicine Peak Quartzite, H = Heart Formation, HQ = Headquarters Schist. x = average, s = one standard deviation.

Table C-2 continued.

	Pelites						Diamictites	
	FS n=6		LS n=4		HQ n=3		HQ n=2	
	x	s	x	s	x	s	x	z
SiO_2	68.55	7.23	79.30	4.01	77.24	10.7	66.55	2.58
TiO_2	0.70	0.21	0.31	0.02	0.40	0.25	0.59	0.04
Al_2O_3	14.32	2.99	11.22	1.73	11.70	4.08	13.70	2.12
Fe_2O_3	6.98	4.98	2.22	0.92	3.39	3.99	7.04	3.00
MgO	1.75	0.70	0.83	0.34	1.24	1.27	2.80	0.78
CaO	0.21	0.03	0.21	0.033	0.75	0.62	2.47	2.17
Na_2O	0.71	0.16	2.72	2.19	2.93	1.56	3.33	2.09
K_2O	4.19	0.46	2.23	0.96	2.24	0.26	2.73	0.86
P_2O_5	0.12	0.026	0.07	0.013	0.08	0.044	0.15	0.03
Rb	136	16.1	85	34.6	81	19.4	113	49.1
Th	10.5	1.2	9.5	2.25	3.5	1.48	6.8	1.1
La	27.8	5.1	39	29.5	7.62	0.36	22.5	4.69
Ta	0.97	0.78	0.58	0.11	0.54	0.24	0.61	0.21
Nb	10	2.13	7	1	5	5.66	7	1.24
Ba	438	266	241	243	229	103	319	1.41
Yb	1.86	0.37	2.62	1.29	0.53	0.04	1.60	0.44
Y	27	3.9	41	30.4	10	5.83	20	8.7
Zr	135	21	213	103	135	37.4	143	7.1
Eu	0.90	0.14	1.22	0.81	0.36	0.04	1.10	0.14
Sr	59	28.6	28	9.2	55	31.3	111	45.3
Sc	11.8	2.84	4.28	2.12	3.54	1.1	14.0	2.83
Co	19.5	8.64	6.1	1.96	7.3	1.08	26.9	111
Ni	34.3	23.7	14.5	1.74	6.4	1.04	49	13.4
Cr	75	32	39	10.1	49	16		

FS = French Slate, LS = Lookout Schist, and HQ = Headquarters Formation. x = average, s = one standard deviation.

REFERENCES

Ball, T. T., and Farmer, G. L., 1991. Identification of 2.0 to 2.4 Ga Nd model age crustal material in the Cheyenne belt, southeastern Wyoming: Implications for Proterozoic accretionary tectonics at the southern margin of the Wyoming craton: Geology, v. 19, p. 360-363.

Blackwelder, E., 1926. Pre-Cambrian geology of the Medicine Bow Mountains: Bull. Geol. Society America, v. 37, p. 615-658.

Blatt, H., 1985. Provenance studies and mudrocks: Jour. Sedimentary Petrol., v. 55, p. 69-75.

Blatt, H. and Sutherland, B., 1969. Intrastratal solution and nonopaque heavy minerals in shales: Jour. Sediment. Petrol., v. 39. p. 591-600.

Boryta, M. and Condie, K. C., 1990. Geochemistry and origin of the Archean Beit Bridge complex, Limpopo Belt, South Africa: Journal of the Geological Society, London, v. 147, p. 229-239.

Carroll, D., 1958. Role of clay minerals in the transportation of iron: Geochim. Cosmochim. Acta, v. 14, p. 1-28.

Chittleborough, D. J., 1991. Indices of weathering for soils and paleosols formed on silicate rocks: Austral. Jour. Earth Sciences, v. 38, p.115-120.

Clayton, J. L., 1986. An estimate of plagioclase weathering rate in the Idaho Batholith based upon geochemical transport rates, in Rates of Chemical Weathering of Rocks and Minerals (eds. Colman, S. T. and D. P. Dothier): Academic Press, Inc., New York, p.453-466.

Condie, K. C., 1991. Another look at rare earth elements in shales: Geochim. Cosmochim. Acta, v. 55, p. 2527-2531.

Condie, K. C., 1992. Sediments and the chemical composition of the upper

continental crust: Revs. Geophys., (in press).

Condie, K. C. and Wronkiewicz, D. J., 1990. The Cr/Th ratio in Precambrian pelites from the Kaapvaal Craton as an index of craton evolution: Earth and Planetary Science Letters, v. 97, p. 256-267.

Cullers, R. L., Barret, T., Carlson, R., and Robinson, B., 1987. Rare-earth and mineralogic changes in Holocene soil and stream sediment: a case study in the Wet Mountains, U. S. A.: Chem. Geol., v. 63, p. 275-297.

Cullers, R. L., 1988. Mineralogical and chemical changes of soil and stream sediment formed by intense weathering of the Danburg Granite, Georgia, U.S.A.: Lithos, v. 21, p. 301-314.

Cullers, R. L., Basu, A. and Suttner, L. J., 1988. Geochemical signature of provenance in sand-size material in soils and stream sediments near the Tobacco Root Batholith, Montana, U.S.A.: Chemical Geology, v. 70, p. 335-348.

Denis, E. and Dabard, M. P., 1988. Sandstone petrography and geochemistry of Late Proterozoic sediments of the Armorican Massif (France)- A key to basin development during the Cadomian Orogeny: Precambrian Research, v. 42, p. 189-206.

Dott, R. H., 1983. The Proterozoic red quartzite enigma in the north-central United States: Resolved by plate collision?: Geol. Society America, Memoir 160, p. 129-141.

Duddy, I. R., 1980. Redistribution and fractionation of rare-earth and other elements in a weathering profile: Chem. Geol., v. 30, p. 363-381.

Duebendorfer, E. M., 1988. Evidence for an inverted metamorphic gradient associated with a Precambrian suture, southern Wyoming: Jour. of Metamorphic Geol., v. 6, p. 41-63.

Duebendorfer, E. M. and Houston, R. S., 1987. Proterozoic accretionary

tectonics at the southern margin of the Archean Wyoming craton: Geol. Society America Bull., v. 98, p. 554-568.

Eade, K. E., and Fahrig, W. F., 1973. Regional. lithological, and temporal variation in the abundances of some trace elements in the Canadian Shield: Geol. Surv. Can. Paper 72-46, 46 pp..

Gibson I. L. and Jagam, P., 1980. Instrumental neutron activation analysis of rocks and minerals, in Mineral. Assoc. Canada Short Course in Neutron Activation Analysis in the Geosciences (ed. G.K. Muecke), p. 109-131.

Govindaraju, K., 1989. Compilation of working values and sample descriptions for 272 geostandards: Geostandards Newsletter, v. 13, p.1-113.

Gromet, L. P., Dymek, R. F., Haskin, L. A. and Korotev, R. L., 1984. The North American shale composite: its compilation, major and trace element characteristics: Geochim. Cosmochim. Acta, v. 48, p. 2469-2482.

Gromet, L. P. and Silver, L. T., 1983. Rare earth element distribution among minerals in a granodiorite and their petrogentic implication: Geochim. Cosmochim. Acta, v. 47, p. 925-939.

Harnois, L., 1988. The CIW index: A new chemical index of weathering: Sedimentary Geol., v. 55, p. 319-322.

Haskin, L. A., Haskin, M. A., Frey, F. A., and Wilderman, T. R., 1968. Relative and absolute terrestrial abundances of the REE, in Origin and Distribution of the Elements: New York, Pergamon, p. 889-912.

Heaman, L. M., Bowins, R., and Crocket, J., 1990. The chemical composition of igneous zircon suites: implication for geochemical tracer studies: Geochim. Cosmochim. Acta, v. 54, p. 1597-1607.

Helmold, K. P., 1985. Provenance of feldspathic sandstones - the effect of diagenesis on provenance interpretations: A review, in Zuffa, G. G., ed., Provenance of Arenites: Amsterdam, D. Reidel, p. 139-163.

Hills, F. A., Gast, P. W., Houston, R. S., and Swainback, I., 1968. Precambrian geochronology of the Medicine Bow Mountains of southeastern Wyoming: Geol. Society America Bull., v. 79, p. 1757-1784.

Hoffman, P. F., 1989. Precambrian geology and tectonic history of North America. DNAG Volume A, Geology of North America - An Overview. Geol. Society America, p. 447-510.

Houston, R. S. and others, 1968. A regional study of rocks of Precambrian age in the part of the Medicine Bow Mountains lying in soouthеastern Wyoming with a chapter on the relationship between Precambrain and Laramide structure: Wyoming Geological Survey Memoir No. 1, 167 p..

Jacobs, J. W., Korotev, R. L., Blanchard, D. P. and Haskin, L. A., 1977. A well-tested procedure for instrumental neutron activation analysis of silicate rocks and minerals: Jour. Radioanal. Chem., v. 40, p. 93-114.

Karlstrom, K. E., Flurkey, A. J., and Houston, R. S., 1983. Stratigraphy and depositional setting of the Proterozoic Snowy Pass Supergroup, southeastern Wyoming: Record of an Early Proterozoic Atlantic-type cratonic margin: Geol. Society America Bull., v. 94, p. 1257-1274.

Kauffman, E. G. and Steidmann, J. R., 1981. Are these the oldest metazoan trace fossils?: Jour. Paleontology, v. 55, p. 923-947.

Lanthier, R., 1979. Stratigraphy and structure of the lower part of the Precambrian Libby Creek Group, central Medicine Bow Mountains, Wyoming: Contributions to Geology, v. 17, p. 135-147.

Lee, D. E. and Bastron, H., 1967. Fractionation of rare-earth elements in allanite and monazite as related to geology of the Mt. Wheeler mine area, Nevada: Geochim. Cosmochim. Acta, v. 31, p. 339-356.

Lindstrom, D. J. and Korotev, R. L., 1982. TEABAGS: Computer programs for instrumental neutron activation analysis: Radioanalyt. Chem., v.70, p. 439-458.

Loubet, M., and Allegre, C. J., 1977. Behaviour of the rare earth elements in the Oklo natural reactor: Geochim. Cosmochim. Acta, v. 41, p. 1539-1548.

Maas, R., and McCulloch, M. T., 1991. The provenance of Archean clastic metasediments in the Narryer Gneiss Complex, Western Australia: Trace element geochemistry, Nd isotopes, and U-Pb ages for detrital zircons: Geochim. Cosmochim. Acta, v. 55, p. 1915-1932.

Marsh, J. S., 1991. REE fractionation and Ce anomalies in weathered Karoo dolerite: Chem. Geol., v. 90, p. 189-194.

Maynard, J. B., Ritger, S. D., and Sutton, S. J., 1991. Chemistry of sands from the modern Indus River and the Archean Witwatersrand basin: Implications for the composition of the Archean atmosphere: Geology, v. 19, p. 265-268.

McBride, E. F., 1985. Diagenetic processes that affect provenance determinations in sandstone, in Zuffa, G. G., ed., Provenance of Arenites: Amsterdam, D. Reidel, p. 95-113.

McLennan, S. M., 1989. Rare earth elements in Sedimentary rocks: Influence of provenance and sedimentary processes: in Geochemistry and Mineralogy of Rare earth Elements, Reviews in Mineralogy, v. 21, p. 169-200.

McLennan, S. M., Fryer, B. J., and Young, G. M., 1979. Rare earth elements in Huronian (Lower Proterozoic) sedimentary rocks: composition and evolution of the post-Kenoran upper crust: Geochim. Cosmochim. Acta, v. 43, p. 375-388.

McLennan, S. M., and Taylor, R. S., 1980. Th and U in sedimentary rocks: crustal evolution and sedimentary recycling: Nature, v. 285, p. 621-624.

McLennan, S. M., Taylor, S. R., McCulloch, M. T., and Maynard, J. B., 1990. Geochemical and Nd-Sr isotopic composition of deep-sea turbidites: Crustal evolution and plate tectonic associations: Geochim. Cosmochim. Acta, v. 54, p.2015-2050.

Michard, A., 1989. Rare earth element systematics in hydrothermal fluids: Geochim. Cosmochim. Acta, v. 53, p. 745-750.

Milliken, K. L., 1988. Loss of provenance information through subsurface diagenesis in Plio-Pleistocene sandstones, northern Gulf of Mexico. Jour. Sedimentary Petrol., v. 58, p. 992-1002.

Milliken, K. L. and Mack, L. E., 1990. Subsurface dissolution of heavy minerals, Frio Formation sandstones of the ancestral Rio Grande Province, South Texas: Sediment. Geology, v. 68, p. 187-199.

Nesbitt, H. W., MacRae, N. D., and Kronberg, B. I., 1990. Amazon deep-sea fan muds: light REE enriched products of extreme chemical weathering: Earth Plan. Science Let., v. 100, p. 118-123.

Nesbitt, H. W., Markovics, G., and Price, R. C., 1980. Chemical processes affecting alkalies and alkaline earths during continental weathering: Geochim. Cosmochim. Acta, v. 44, p. 1659-1666.

Nesbitt, H. W. and Young, G. M., 1982. Early Proterozoic climates and plate motions inferred from major element chemistry of lutites: Nature, v. 299, p. 715-717.

Norrish K. and Chappel B. W., 1977. X-ray fluorescence spectrometery, in Physical Methods in Determinative Minerology (ed. J. Zussman), p. 235-237 and 257-262. Academic Press, New York.

Norrish, K. and Hutton, J. T., 1969. An accurate x-ray spectrographic

method for the analysis of a wide range of geological samples: Geochim. Cosmochim. Acta, v.33, p.431-453.

Peterman, Z. E. and Hildreth, R. A., 1978. Reconnaissance geology and geochronology of the Precambrian of the Granite Mountains, Wyoming: U.S. Geol. Survey Professional Paper 1055, 22 p..

Pettijohn, F. J., 1941. Persistence of heavy minerals and geologic age: Jour. Geology: v. 49, p. 612-625.

Pettijohn, F. J., Potter, P. E., and Siever, R., 1973. Sand and Sandstone: New York, Springer-Verlag, 618 p..

Pittman, E. D.,1979. Recent advances in sandstone diagenesis: Ann. Rev. Earth Planet. Sci., v. 7, p.39-62.

Premo, W.R. and Van Schmus, W.R., 1989. Zircon geochronology of Precambrian rocks in southeastern Wyoming and northern Colorado: Geol. Society America Special Paper 235, p. 13-32.

Roscoe, S. M., 1989. The reappearance of the Huronian in Wyoming: Geol. Society America, Abst. With Programs, v. 23, p. 373.

Sawka, W. N., 1988. REE and trace element variations in accessory minerals and hornblende from the strongly zones McMurry Meadows pluton, California: Trans. Royal Society Edinburgh: Earth Sciences, v. 76, p. 411-449.

Sawyer, E. W., 1986. The influence of source-rock type, chemical weathering and sorting on the geochemistry of clastic sediments from the Quetico Metasedimentary Belt, Superior Province, Canada: Chem. Geol., v. 55, p. 77- 95.

Schau, M., and Henderson, J. B., 1983. Archean chemical weathering at three localities on the Canadian Shield: Prec. Res., v. 20, p. 189-224.

Shaw, D. M., Dostal, J., and Keays, R. R., 1976. Additional estimates of continental surface Precambrian shield composition in Canada: Geochim. Cosmochim. Acta, v. 40, p. 73-83.

Stuckless, J. S., Hedge, C. E., Worl, R. G., Simmons, K. R., Nkomo, I. T., and Wenner, D. B., 1985. Isotopic studies of the Late Archean plutonic rocks of the Wind River Range, Wyoming: Geol. Society America Bull., v. 96, p. 850-860.

Taylor, S. R., and McLennan, S. M., 1983. Geochemistry of Early Proterozoic sedimentary rocks and the Archean/Proterozoic boundary: Geol. Society America Memoir 161, p. 119-130.

Taylor, S. R. and McLennan, S. M., 1985. The Continental Crust: its composition and evolution: Boston, Blackwell Scientific Publications, 312 p..

van de Kamp, P. C. and Leake, B. E., 1986. Petrography and geochemistry of feldspathic and mafic sediments of the northeastern Pacific margin: Trans. Royal Society Edinburgh: Earth Sciences, v. 76, p. 411-449.

Wronkiewicz, D. J. and Condie, K. C., 1987. Geochemistry of Archean shales from the Witwatersrand Supergroup, South Africa: Source-area weathering and provenance: Geochim. Cosmochim. Acta, v. 51, p. 2401-2416.

Wronkiewicz, D. J., and Condie, K. C., 1989. Geochemistry and provenance of sediments from the Pongola Supergroup, South Africa: Evidence for a 3.0 Ga old continental craton: Geochim. Cosmochim. Acta, v. 53, p. 1537-1549.

Wronkiewicz, D. J. and Condie, K. C., 1990. Geochemistry and mineralogy of sediments from the Ventersdorp and Transvaal Supergroups, South Africa: Cratonic evolution during the Early Proterozoic: Geochim. Cosmochim. Acta, v. 54, p. 343-354.

Young, G. M., 1970. An extensive Early Proterozoic glaciation in North America?: Paleogeograph. , Paleoclimatol., Paleoecol. v. 7, p. 85-101.

Young, G. M., 1973. Tillites and aluminous quartzites as possible time markers for Middle Precambrian (Aphebian) rocks of North America: The Geological Association of Canada Special Paper 12, p. 97-127.